A Photoaffinity Displacement Assay and Probes to Study the Cyclin-Dependent Kinase Family

Emma K. Grant,[a,b] David J. Fallon,[a,b] H. Christian Eberl,[c] Ken G. M. Fantom,[a] Francesca Zappacosta,[d] Cassie Messenger,[a] Nicholas C. O. Tomkinson[b] and Jacob T. Bush*[a]

[a] E.K. Grant, D.J. Fallon, K.G.M. Fantom, C. Messenger, Dr. J.T. Bush GlaxoSmithKline, Gunnels Wood Road, Stevenage, Hertfordshire, SG1 2NY, UK
E-mail: jacob.x.bush@gsk.com
[b] E.K. Grant, D.J. Fallon, Prof. N.C.O. Tomkinson, Department of Pure and Applied Chemistry, University of Strathclyde, 295 Cathedral Street, Glasgow, G1 1XL, UK
[c] Dr. H.C. Eberl, Cellzome GmbH, a GSK company, Meyerhofstraße 1, Heidelberg 69117, Germany
[d] Dr. F. Zappacosta , GlaxoSmithKline, South Collegeville Road, Collegeville, PA 19426, U.S

Abstract: The CDK family plays a crucial role in the control of the cell cycle. Dysregulation and mutation of the CDKs has been implicated in cancer and the CDKs have been investigated extensively as potential therapeutic targets. Selective inhibition of specific isoforms of the CDKs is crucial to achieve therapeutic effect while minimising toxicity. We present a group of photoaffinity probes designed to bind to the family of CDKs. The site of crosslinking of the optimised probe, as well as its ability to enrich members of the CDK family from cell lysates, was investigated. In a proof of concept study, we subsequently developed a photoaffinity probe-based competition assay to profile CDK inhibitors. We anticipate that this approach will be widely applicable to the study of small molecule binding to protein families of interest.

Introduction

Photoaffinity probes have proved useful tools for the capture of reversible small molecule-protein interactions. They have been used for profiling changes in protein expression levels to investigate the biological origin of phenotypic changes,[1] and in the determination of inhibitor selectivity profiles.[2-4] Photoaffinity probes typically consist of three functionalities (Figure 1A): the selectivity function, which binds to the target of interest; the photoreactive group, which will crosslink to bound protein; and the bioorthogonal handle for downstream workflows.[5-6] The design of the probe, including choice of photoreactive group, profoundly impacts the likelihood of successful protein capture. There have been few studies to systematically compare the efficiency of crosslinking of commonly used photoreactive groups and there is still no consensus on the ideal photoreactive group and attachment strategy.[7-9] Biochemical studies into the determinants of crosslinking yields will help inform on the design of photoaffinity probes for applications of interest.

Since the concept of photoaffinity labelling (PAL) was first introduced in the 1960's,[10] many PAL applications have evolved, such as performing fragment screening in live cells with fully functionalised fragments (FFFs) and activity-based protein profiling (ABPP),[1, 11-12] and many more developments can be envisioned based on affinity-based workflows (e.g. kinobeads).[13] Expansion of photoaffinity methodologies, including optimisation of probes for therapeutically important protein families, as well as the development of novel technical applications, will likely provide valuable tools for the study of biological systems.

The cyclin-dependent kinases (CDKs) are fundamental in the regulation of the cell cycle.[14-17] Due to their role in cell proliferation, CDKs are heavily implicated in cancers, where they are often found to be mutated.[18-19] Selective inhibition of specific isoforms of the CDKs is crucial to achieve therapeutic effect while minimising toxicity.[20-24] Recently, oncolytic clinical efficacy has been achieved with CDK4/6 inhibitors: palbociclib, ribociclib and abemaciclib.[25] Photoaffinity probes for

the CDK family could aid studies to further understand the role of these proteins in the cell cycle and cancer, and also be used to profile inhibitor selectivity.

Herein we report a group of 12 photoaffinity probes designed to crosslink to the CDK family. Crosslinking studies with CDK2, CDK7 and CDK9 were conducted to identify the probe with the optimal profile, and LC-MS/MS experiments were used to investigate the site of crosslinking. The best probe enabled enrichment of CDK proteins from cell lysates, offering a tool for the study of the family. Subsequently, this probe was used as a reporter ligand in a biochemical MS-based competition assay to measure the potency of CDK inhibitors. This approach was straightforward to implement and could be applied to other protein families by selection of a suitable ligand.

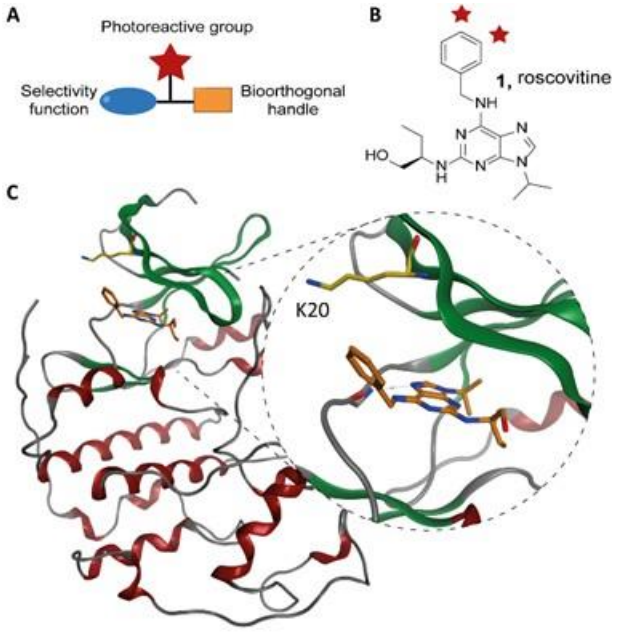

Figure 1: A: Generic structure of a photoaffinity chemical probe. **B:** Structure of pan-CDK inhibitor roscovitine (**1**), highlighting attachment points for photoaffinity groups. **C**: Crystal structure (PDB ID: 2A4L) of roscovitine in complex with CDK2.

Results and Discussion

The pan-CDK inhibitor roscovitine was used as the selectivity function in the design of a photoaffinity probe for the CDK family (Figure 1B).[26] A crystal structure of roscovitine in complex with CDK2 indicated that the phenyl ring is solvent exposed (PDB ID: 2A4L, Figure 1C). We postulated that introduction of a photoaffinity group in the meta or para position of this ring might minimise the effect on reversible binding while enabling crosslinking to occur. Initially, ten probes (P1-P10) were designed and synthesised, incorporating five commonly used photoreactive groups at two attachment points, to identify which would give the best crosslinking to CDK proteins (Figure 2A/B, for synthesis see Figure S1). To confirm the photoaffinity groups did not preclude binding of the selectivity function to the active site, pIC50 values of the probes against CDK2, CDK7 and CDK9 were measured using an ADP-GloTM assay (Figure 2B).[27] All probes were found to have similar potency to roscovitine at the three CDKs (pIC50 = 6 – 7.1, roscovitine pIC50 = 6.4 – 6.7) indicating that the photoreactive groups in both the meta or para positions could be accommodated by the proteins, and should be optimally positioned to enable crosslinking, given their short linkers. The physicochemical properties of the probes were also measured to investigate the influence of the various photoreactive groups (Figure S2). Overall, the alkyl diazirines P7 and P8 gave the smallest shift in physicochemical properties relative to the parent roscovitine.

A

B

	CDK2	CDK7	CDK9
roscovitine	6.7± 0.03	6.6±0.05	6.4± 0.02
P1 *(m)*	6.8 ± 0.06	6.6 ± 0.11	6.7 ± 0.06
P2 *(p)*	7.0 ± 0.17	6.6 ± 0.21	6.9 ± 0.11
P3 *(m)*	6.9 ± 0.11	6.3 ± 0.02	6.9 ± 0.01
P4 *(p)*	6.9 ± 0.25	6.9 ± 0.35	6.9 ± 0.01
P5 *(m)*	7.0 ± 0.04	6.4 ± 0.07	6.8 ± 0.13
P6 *(p)*	6.7 ± 0.00	6.0 ± 0.23	6.7 ± 0.01
P7 *(m)*	6.5 ± 0.06	6.3 ± 0.04	6.4 ± 0.05
P8 *(p)*	6.7 ± 0.11	6.0 ± 0.15	6.4 ± 0.03
P9 *(m)*	6.8 ± 0.06	6.5 ± 0.13	7.1 ± 0.01
P10 *(p)*	6.6 ± 0.01	6.5 ± 0.03	7.0 ± 0.12

Figure 2: A: Final step in the synthesis of 10 photoaffinity probes (**P1-P10**), introducing the photoreactive groups to the *meta* and *para* positions of roscovitine. **B:** Inhibition data (pIC_{50}) for probes **P1**-**P10** against CDK2, CDK7 and CDK9, as determined by ADP-Glo™ assay (n=2, one standard deviation).

The crosslinking yields of probes P1-P10 were investigated upon irradiation with CDK2, CDK7 and CDK9 proteins. Probes were used at a concentration above their IC50 values to ensure complete binding. Thus, probes (P1-P10, 2 µM) were incubated with recombinant protein (1 µM, 15 min, 4 °C) before irradiation (302 nm, 10 min) and analysis by intact mass spectrometry (Figure 3A). Crosslinking could be determined by the presence of a peak corresponding to the mass of protein+probe (see *, Figure 3B/3C). In some cases, an additional mass shift of +16 or +32 was observed (e.g. P3 and P4), which likely corresponds to oxidation following quenching of a reactive intermediate with water. Crosslinking yields were approximated from the ratio of the area under peaks corresponding to protein and protein+probe (Figure 3D). The aryl azide, tetrafluoroaryl azide and alkyl diazirine probes (P1-P4, P7 and P8) gave good crosslinking yields across the three proteins (9-35%). The trifluoromethyl diazirines (P5 and P6) showed little or no crosslinking with the three proteins (≤8%), which is perhaps surprising given its extensive use in photolabelling studies.[28] Benzophenones (P9 and P10) gave good crosslinking to CDK9 (40% and 53%), but no significant crosslinking to CDK2 and CDK7. Benzophenones have been reported to preferentially crosslink to methionine residues, therefore crosslinking to CDK9 may occur to a proximal methionine (M308) which is absent in CDK2 and CDK7 (Figure S4).[29] Irradiation of probes P1-P10 with CDK2 at 365 nm, thought to be more suited to benzophenones and diazirines, did not show any improvement in crosslinking yield (Figure S3).[4] There were no significant variations in crosslinking yields between the meta and para substituted probes suggesting that both vectors placed the photoreactive groups in sufficient proximity to the protein to enable crosslinking.

To explore photocapture of CDKs from lysates, optimal probes were selected for incorporation of an alkyne as a bioorthogonal handle. The alkyl diazirines (P7 and P8) were selected as these showed good crosslinking to all three CDK isoforms. In addition, P7 and P8 had high solubility and low lipophilicity,

which should minimise non-specific protein binding. The aryl azides (P1-P4) also gave good crosslinking, however the nitrene intermediate has been reported to undergo rearrangements leading to non-specific crosslinking.[30] Alkyne functionalised diazirine probes P11 and P12 were synthesised and found to exhibit similar potencies to the parent roscovitine at CDK2, CDK7 and CDK9 (Figure 4, for synthesis and physicochemical data see Figure S1 and Figure S2). The crosslinking of probes P11 and P12 to CDK2, CDK7 and CDK9 were investigated as described above, and gave good yields (Figure 4D, >12%). Representative mass spectra for P11 and P12 crosslinking to CDK2 are shown with the expected mass position of the protein+probe peak indicated (Figure 4C). The para-substituted probe P12 gave higher crosslinking yields (CDK2=15%, CDK7=41% and CDK9=34%) suggesting the diazirine is better positioned to interact with a residue of the protein.

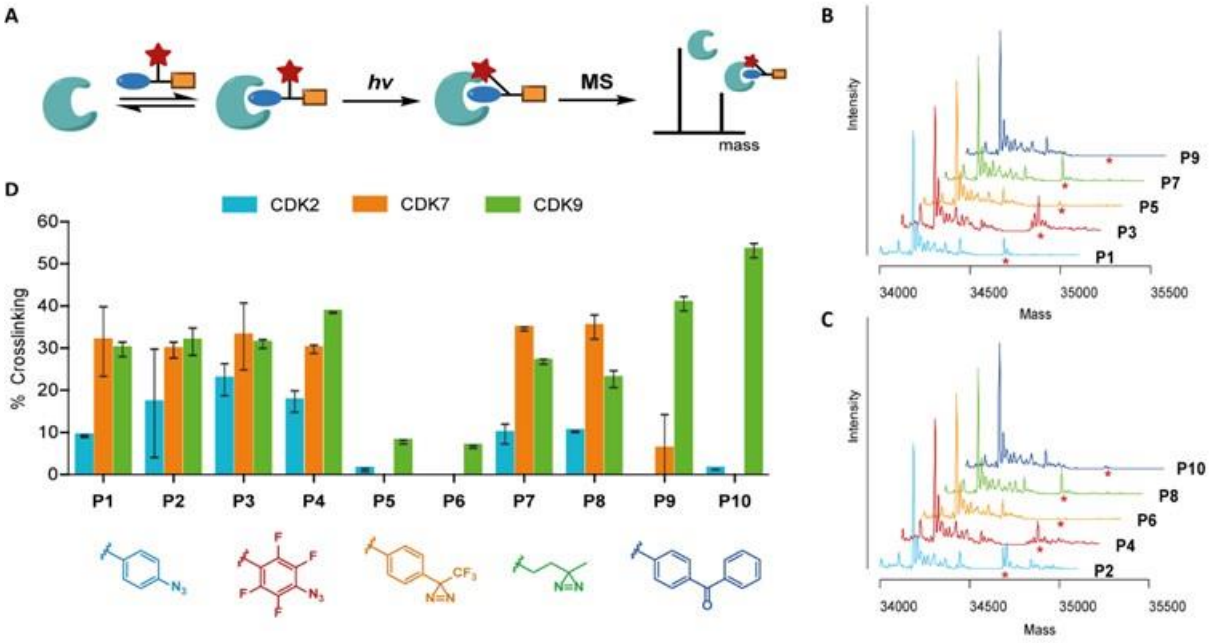

Figure 3: **A**: Schematic of workflow used to measure crosslinking yields. **B/C**: Intact MS (ESI-TOF) spectra of meta (B) and para probes (C) after irradiation with CDK2 recombinant protein. (*) indicates expected mass of protein+probe. **D**: Crosslinking yields of probes P1-P10 (2 µM) with recombinant proteins CDK2, CDK7 and CDK9 (1 µM) following irradiation with UV light (302 nm, 10 min). Error bars indicate standard deviation over two replicates.

The site of crosslinking of probe P12 with recombinant CDK2 was investigated by tryptic digest and tandem LC-MS/MS analysis. Probe P12 (6 µM) or DMSO control, were incubated with CDK2 (3 µM) before UV irradiation (302 nm, 5 min). The protein was then reduced, treated with iodoacetamide, and digested using trypsin. Digests were analysed by LC-MS/MS (Q-ExactiveTM) and a database search was performed including the mass of probe-N2 on any residue as a variable modification. The tryptic peptide 10IGEGTYGVVYK*AR22 was identified carrying a modification on K20, which was not observed in the DMSO control sample (Figure 4E). This finding is corroborated by a co-crystal structure of roscovitine with CDK2 suggesting that K20 would be ideally situated to interact with the carbene intermediate extending from the para position (Figure 1C, PDB ID: 2A4L).

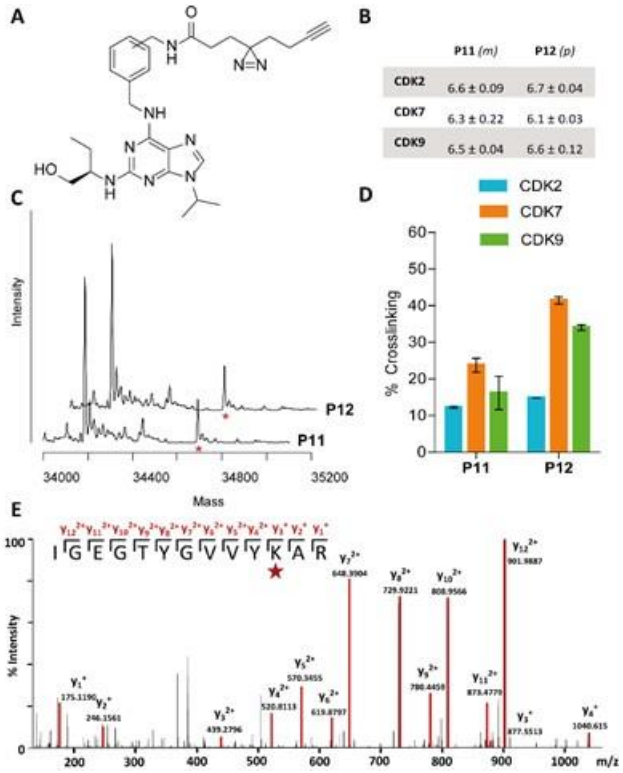

Figure 4: A: Structure of alkyne-functionalised diazirine probes **P11** and **P12**. **B**: Inhibition data (pIC_{50}) of **P11** and **P12** against CDK2, CDK7 and CDK9 as determined by ADP-Glo™ assay (n=2, one standard deviation). **C**: Intact MS spectra (ESI-TOF) following irradiation of **P11** and **P12** with CDK2 recombinant protein, (*) indicates the expected mass of protein+probe. **D**: Crosslinking yields upon irradiation (302 nm, 10 min) of **P11** and **P12** (2 µM) with recombinant proteins CDK2, CDK7 and CDK9 (1 µM). Error bars indicate standard deviation over two replicates. **E:** LC-MS/MS spectrum of the trypsin-derived peptide $_{10}$IGEGTYGVVYK*AR$_{22}$ crosslinked to **P12** indicating K20 as the site of crosslinking.

The application of probe P12 for the capture of CDK proteins from cell lysates was subsequently investigated. HL-60 cell lysates were treated with probe P12 (10 µM), or P12 (10 µM) and a competitor compound 9 (200 µM, Figure S1). The samples were incubated at 4 °C for 1 h before irradiation with UV light (302 nm, 10 min). P12-modified proteins were reacted with azidobiotin by copper-mediated cycloaddition. Excess CuAAC reagents were removed by acetone precipitation, and the proteins were resolubilised. Biotinylated proteins were enriched using neutravidin beads before on-bead tryptic digestion. The resulting peptides were labelled with isobaric mass tags (TMT4) and analysed by tandem mass spectrometry (Figure 5A).[31]

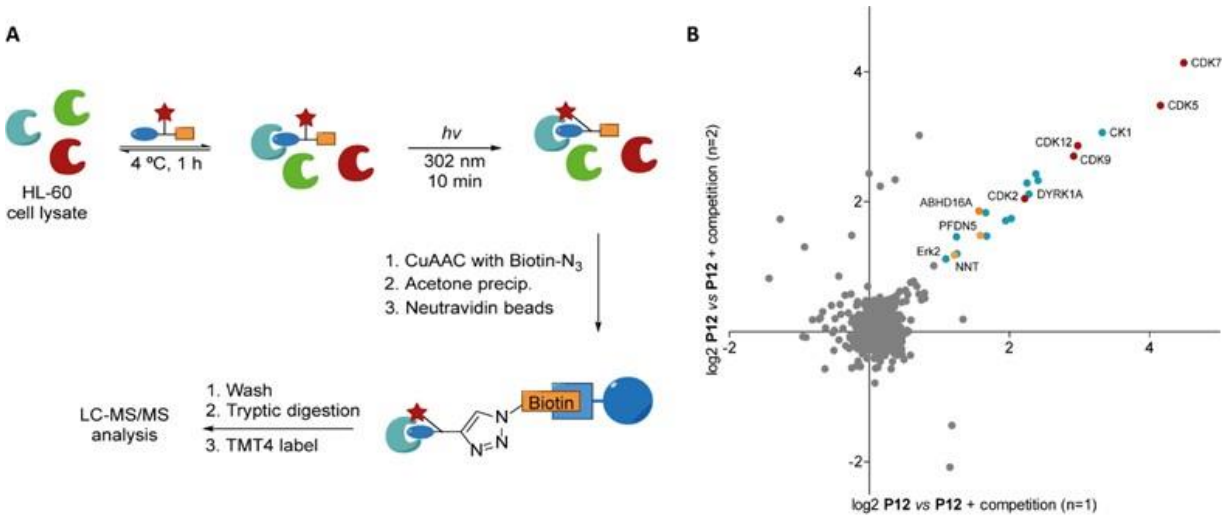

Figure 5: A: Schematic workflow of MS-based proteomic experiments to identify proteins enriched by photoaffinity probe **P12**. **B:** Plot of the proteins that were enriched by **P12**. Proteins that were competed by **9** are highlighted: red – CDKs, blue – other kinases, orange – non-kinase.

Roscovitine-based probe P12 enriched 20 proteins that were competitively displaced by the parent compound 9. This included five members of the CDK family (CDK2, CDK5, CDK7, CDK9 and CDK12). Of the five CDKs identified, roscovitine has been reported to inhibit CDK2, CDK5, CDK7 and CDK9 with IC50 values of <1 µM.[24] A further 12 kinases and three non-kinases were also selectively enriched (Figure 5B, for kinome map see Figure S5). A previous study on kinase off-targets of roscovitine using biochemical assays identified three of these off-targets, DYRK1a, ERK2 and CK1.[32] The further nine kinases recognised here may represent additional off-targets of roscovitine. Three previously unidentified non-kinase targets were also enriched, hydrogenase NNT,[33] chaperone PFDN5[34] and hydrolase ABHD16A.[35] This study highlights the utility of P12 for profiling the selectivity of CDK inhibitors. Further optimisation is in progress to increase the coverage of the CDK family and to enable application in live cells.

We envision that photoaffinity probes, such as P12, can be used as reporter ligands in biochemical MS-based competition assays to enable the profiling of inhibitors. In this approach, the protein is incubated with a photoaffinity probe and an inhibitor of interest to establish a competitive binding equilibrium before irradiation. Variation of inhibitor concentration causes a dose dependent reduction in crosslinking, enabling calculation of IC50 values (Figure 6A).

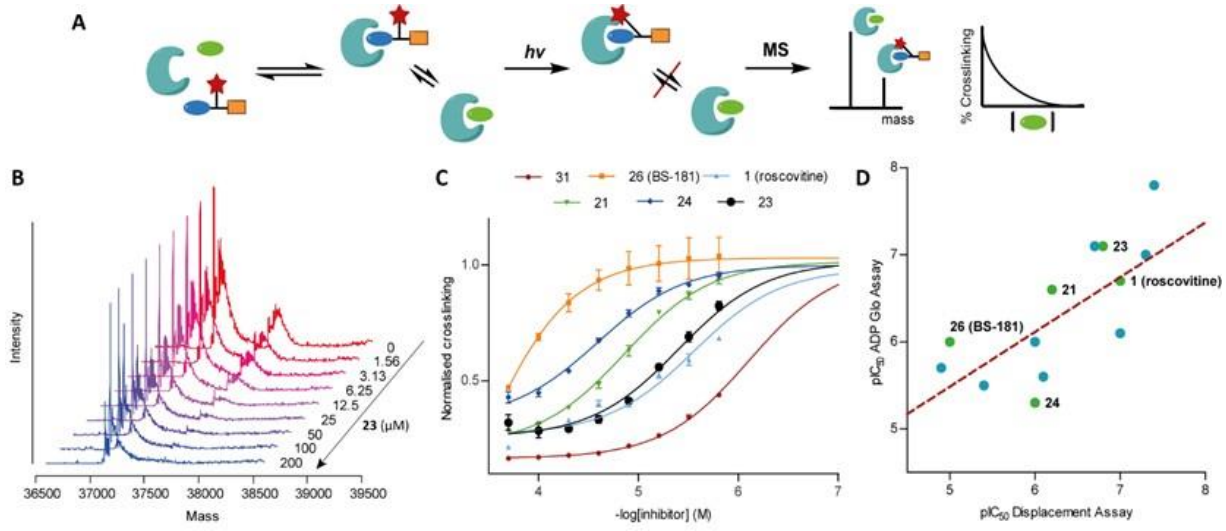

Figure 6: A: Schematic of workflow of a photoaffinity probe-based displacement assay. CDK2 and **P12** are incubated with increasing concentrations of competitive inhibitor. Irradiation freezes the equilibrium and crosslinking yields are determined by MS. **B:** Overlay of intact mass spectra following irradiation of CDK2 and **P12** (5 μM) in the presence of competitive inhibitor **23** (0 – 200 μM). **C:** Dose response curves generated for six compounds analysed by displacement assay. Normalised crosslinking yield of **P12**+CDK2 is plotted against -log[inhibitor](M) (n=3). **D:** Comparison of pIC_{50} values generated by displacement assay (n=3) versus ADP-Glo™ assay (n=2) for 14 compounds (an additional six compounds showed pIC_{50} values above the limit of the assay, corrected >7.4). Line of best fit in red, R^2=0.5.

A selection of 20 known CDK inhibitors (1 and 17-35) were chosen for a proof of concept study against CDK2 (Figure S6). This group of inhibitors included compounds that have reached clinical trials: roscovitine, flavopiridol, BS-181 and R547.[23, 36-37] P12 was used at 5 μM to be both above the concentration of the protein (1 μM) and above its KD (pIC50 = 6.7, ADP-GloTM), to ensure complete binding. A range of concentrations of the free inhibitor (200 μM – 1.56 μM) were incubated with CDK2 and P12, before irradiation with UV light, and analysis by intact MS to determine crosslinking yields. Consistent with competitive displacement, the [P12+CDK2] crosslinking yield was found to decrease with increasing inhibitor concentration, with good reproducibility across three replicates (Figure 6B). Crosslinking yields were normalised to the DMSO control and pIC50 values were derived from plots of -log[inhibitor] (M) vs response (Figure 6C). The data points exhibited low standard deviation and followed the expected one-site competition binding model. Potency values varied from pIC50 3.5 – 6. These values will be dependent on the KD and concentration of the photoaffinity probe used, and therefore the assay can be tailored to a required range of sensitivity. As validation of the assay, the 20 inhibitors were also screened in the ADP-GloTM assay. The pIC50 values generated from the displacement assay were corrected using the Cheng-Prusoff equation, based on the ADP-GloTM-derived pIC50 value of P12 (SI Table 13). The assays show good correlation, particularly given their different formats: competitive binding vs enzyme activity (Figure 6D). An advantage of this assay over other binding assays (e.g. SPR, thermal shift), is that it measures binding to a specific site on the protein. A particularly exciting extension of this approach is the potential for application in live cells.[1] Currently, the approach is limited by the sensitivity of the MS analysis, requiring high concentrations of protein and thereby narrowing the dynamic range that can be measured. Use of superior analytical instrumentation may allow improvement in sensitivity, and variation in probe concentration or KD could increase the dynamic range. Additionally, higher throughput analytical instrumentation (e.g. RapidFire®, ~10 seconds per sample) might offer a means to scale the assay.

Conclusion

In summary, we describe a family of pan-CDK photoaffinity probes based on the pan-CDK inhibitor roscovitine. The variations observed in the crosslinking yields of the probes to CDK2, CDK7 and CDK9, highlight the challenges associated with the design of an 'ideal' probe and support the synthesis of a selection of probes in order to obtain reliable protein capture.[7, 38-39] In this case, the optimal probes contained alkyl diazirines which were elaborated to include an alkyne bioorthogonal handle (P11/P12). LC-MS/MS analysis of P12+CDK2 revealed the site of crosslinking. In proteomic MS studies with cell lysates, P12 was found to enrich five CDKs as well as 12 other kinases. Further optimisation is ongoing to improve the coverage of the CDK family and to enable application in live cells, where probes could offer application in comparing CDK expression levels across phenotypes and disease states. Probe P12 was subsequently used in a proof of concept study to enable profiling of inhibitors by competitive displacement. This approach was validated by determining the pIC50 values of a selection of known CDK inhibitors which correlated with data from an ADP-GloTM assay. We anticipate

that this could provide a complementary approach to other binding assays, with the advantage of providing a measurement of site-specific binding for any ligandable protein pocket.

Experimental Section

Biological methods, synthetic methods and characterisation, and supplementary Figures S1-S6. Supplementary proteomic data set.

Acknowledgements

We would like to thank the GlaxoSmithKline/University of Strathclyde Collaborative PhD programme for funding this work. We thank D. Price for crystallographic analysis, J. Stuhlfauth and N. Garcia-Altrieth for cell lysate preparation and K. Kammerer for LC MS/MS analysis. Many thanks to M.M. Hann, M. Barker and B. Cosgrove for proofreading of the manuscript. We thank the EPSRC for funding via Prosperity Partnership EP/S035990/1, the SCI for funding via a 2018 Scholarship (EKG) and the Scottish Funding Council for a Postgraduate and Early Career Researcher Exchanges (PECRE) grant (H17014) (DJF).

References

[1] C. G. Parker, A. Galmozzi, Y. Wang, B. E. Correia, K. Sasaki, C. M. Joslyn, A. S. Kim, C. L. Cavallaro, R. M. Lawrence, S. R. Johnson, I. Narvaiza, E. Saez, B. F. Cravatt, *Cell* **2017**, *168*, 527-541.

[2] S. Pan, S. Y. Jang, D. Wang, S. S. Liew, Z. Li, J. S. Lee, S. Q. Yao, *Angew. Chem., Int. Ed. Engl.* **2017**, *56*, 11816-11821.

[3] P. Kleiner, W. Heydenreuter, M. Stahl, V. S. Korotkov, S. A. Sieber, *Angew. Chem., Int. Ed. Engl.* **2017**, *56*, 1396-1401.

[4] J. G. Lumb, M. W. Halloran, *Chem. Eur. J.* **2019**, *25*, accepted Nov 2018.

[5] H. Guo, Z. Li, *Med. Chem. Comm.* **2017**, *8*, 1585-1591.

[6] D. J. Lapinsky, *Fut. Med. Chem.* **2015**, *7*, 2143-2171.

[7] J. T. Bush, L. J. Walport, J. F. McGouran, I. K. H. Leung, G. Berridge, S. S. van Berkel, A. Basak, B. M. Kessler, C. J. Schofield, *Chem. Sci.* **2013**, *4*, 4115-4120.

[8] A. R. Sherratt, N. Nasheri, C. S. McKay, S. O'Hara, A. Hunt, Z. Ning, D. Figeys, N. K. Goto, J. P. Pezacki, *ChemBioChem* **2014**, *15*, 1253-1256.

[9] G. F. Desrochers, C. Cornacchia, C. S. McKay, J. P. Pezacki, *ACS. Infect. Dis.* **2018**, *4*, 752-757.

[10] A. Singh, E. R. Thorton, F. H. Westheimer, *J. Biol. Chem.* **1962**, *237*, PC3006-PC3008.

[11] A. Saghatelian, N. Jessani, A. Joseph, M. Humphrey, B. F. Cravatt, *PNAS* **2004**, *101*, 10000-10005.

[12] Q. Zhao, X. Ouyang, X. Wan, K. S. Gajiwala, J. C. Kath, L. H. Jones, A. L. Burlingame, J. Taunton, *J. Am. Chem. Soc.* **2017**, *139*, 680-685.

[13] M. Bantscheff, D. Eberhard, Y. Abraham, S. Bastuck, M. Boesche, S. Hobson, T. Mathieson, J. Perrin, M. Raida, C. Rau, V. Reader, G. Sweetman, A. Bauer, T. Bouwmeester, C. Hopf, U. Kruse, G. Neubauer, N. Ramsden, J. Rick, B. Kuster, G. Drewes, *Nat Biotechnol* **2007**, *25*, 1035-1044.

[14] M. Malumbres, E. Harlow, T. Hunt, T. Hunter, J. M. Lahti, G. Manning, D. O. Morgan, L. H. Tsai, D. J. Wolgemuth, *Nat. Cell. Biol.* **2009**, *11*, 1275-1276.

[15] G. I. Shapiro, *J. Clin. Oncol.* **2006**, *24*, 1770-1783.

[16] S. Lim, P. Kaldis, *Development* **2013**, *140*, 3079-3093.

[17] C. Sanchez-Martinez, L. M. Gelbert, M. J. Lallena, A. de Dios, *Bioorg. Med. Chem. Lett.* **2015**, *25*, 3420-3435.

[18] M. Malumbres, M. Barbacid, *Nat. Rev. Cancer.* **2009**, *9*, 153-166.

[19] M. Peyressatre, C. Prevel, M. Pellerano, M. C. Morris, *Cancers (Basel)* **2015**, *7*, 179-237.

[20] J. Cicenas, M. Valius, *J. Cancer. Res. Clin. Oncol.* **2011**, *137*, 1409-1418.

[21] D. Parry, T. Guzi, F. Shanahan, N. Davis, D. Prabhavalkar, D. Wiswell, W. Seghezzi, K. Paruch, M. P. Dwyer, R. Doll, A. Nomeir, W. Windsor, T. Fischmann, Y. Wang, M. Oft, T. Chen, P. Kirschmeier, E. M. Lees, *Mol. Cancer. Ther.* **2010**, *9*, 2344-2353.
[22] N. Raje, P. N. Hari, H. Landau, P. G. Richardson, J. Rosenblatt, N. Couture, J. F. Lyons, G. Langford, M. Yule, *ASH Annual Meeting Abstract* **2013**.
[23] S. Diab, S. Eckhardt, A. Tan, G. Frenette, L. Gore, W. Depinto, J. Grippo, M. DeMario, S. Mikulski, S. Papadimitrakopoulou, *J. Clin. Oncol.* **2016**, *25*, 3528-3528.
[24] U. Asghar, A. K. Witkiewicz, N. C. Turner, E. S. Knudsen, *Nat. Rev. Drug. Discov.* **2015**, *14*, 130-146.
[25] S. Goel, M. J. DeCristo, S. S. McAllister, J. J. Zhao, *Trends Cell. Biol.* **2018**, *28*, 911-925.
[26] J. Cicenas, K. Kalyan, A. Sorokinas, E. Stankunas, J. Levy, I. Meskinyte, V. Stankevicius, A. Kaupinis, M. Valius, *Ann. Transl. Med.* **2015**, *3*, 135-147.
[27] P. Corporation, **2015**.
[28] E. Smith, I. Collins, *Fut. Med. Chem.* **2015**, *7*, 159-183.
[29] A. Wittelsberger, B. E. Thomas, D. F. Mierke, M. Rosenblatt, *FEBS Lett.* **2006**, *580*, 1872-1876.
[30] Y. Li, J. P. Kirby, M. W. George, M. Poliakoff, G. B. Schuster, *J. Am. Chem. Soc.* **1988**, *110*, 8092-8098.
[31] L. Dayon, A. Hainard, V. Licker, N. Turck, K. Kuhn, D. F. Hochstrasser, P. R. Burkhard, J. Sanchez, *Anal. Chem.* **2008**, *80*, 2921-2931.
[32] S. Bach, M. Knockaert, J. Reinhardt, O. Lozach, S. Schmitt, B. Baratte, M. Koken, S. P. Coburn, L. Tang, T. Jiang, D. C. Liang, H. Galons, J. F. Dierick, L. A. Pinna, F. Meggio, F. Totzke, C. Schachtele, A. S. Lerman, A. Carnero, Y. Wan, N. Gray, L. Meijer, *J. Biol. Chem.* **2005**, *280*, 31208-31219.
[33] E. Meimaridou, J. Kowalczyk, L. Guasti, C. R. Hughes, F. Wagner, P. Frommolt, P. Nurnberg, N. P. Mann, R. Banerjee, H. N. Saka, J. P. Chapple, P. J. King, A. J. Clark, L. A. Metherell, *Nat. Genetics* **2012**, *44*, 740-742.
[34] I. E. Vainberg, S. A. Lewis, H. Rommelaere, C. Ampe, J. Vandekerckhove, H. L. Klein, N. J. Cowan, *Cell* **1998**, *93*, 863-873.
[35] T Spies, G. Blanck, M Bresnahan, J. Sands, J. L. Strominger, *Science* **1989**, *243*, 214-217.
[36] A. M. Senderowicz, *Invest. New Drugs* **1999**, *17*, 313-320.
[37] B.-Y. Wang, Q.-Y. Liu, J. Cao, J.-W. Chen, Z.-S. Liu, *Drug. Des. Dev. Ther.* **2016**, *10*, 1181-1189.
[38] K. Sakurai, S. Ozawa, R. Yamada, T. Yasui, S. Mizuno, *Chem. Biochem.* **2014**, *15*, 1399-1403.
[39] P. A. J. Weber, A. G. Beck-Sickinger, *J. Peptide Res.* **1997**, *49*, 375-383

Table of Contents

1. Supplementary figures

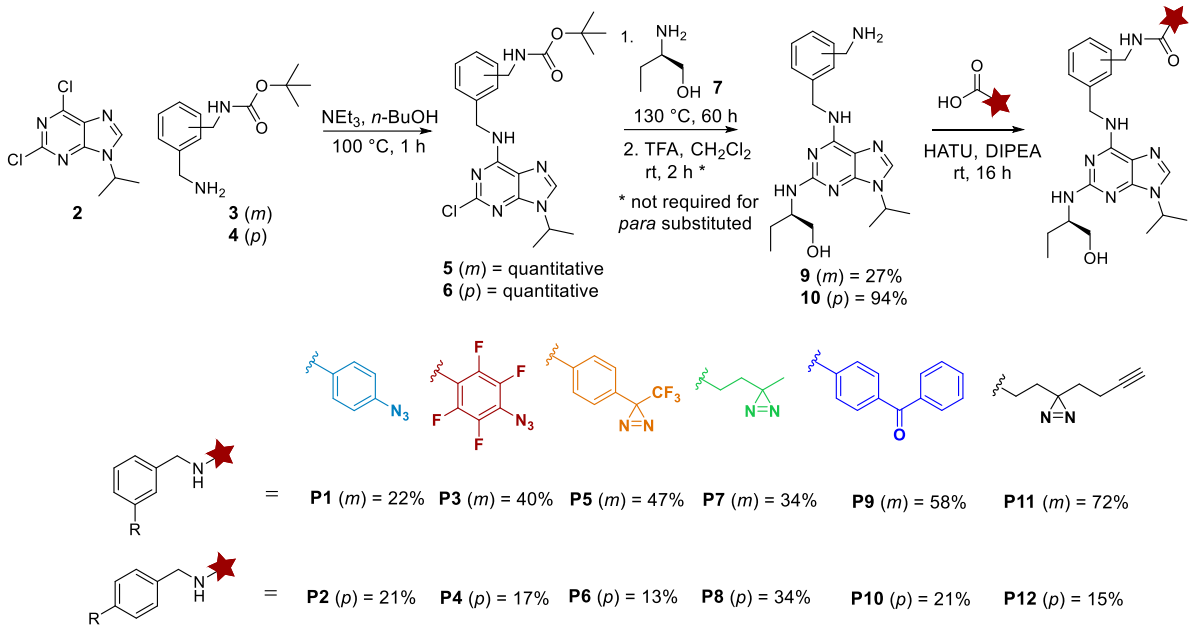

Figure S1: Synthesis of photoaffinity probes (**P1-P12**).

Compound	ChromLogD$_{7.4}$	HSA/AGP (%)	Aqu. Kinetic Solubility (µM)	Permeability (nm/s)
roscovitine	4.54	91/82	467	620
P1	4.95	96/87	46	340
P2	4.84	97/85	31	290
P3	5.56	96/87	28	250
P4	5.48	97/85	25	360
P5	6.23	97/90	18	220
P6	6.13	97/90	<1	310
P7	4.23	89/83	>450	400
P8	4.08	94/77	227	330
P9	5.43	96/89	19	380
P10	5.31	97/89	<1	300
P11	4.67	93/85	144	440
P12	4.54	95/83	91	340

Figure S2: Physicochemical data for photoaffinity probes (**P1-P12**). HSA – human serum albumin and AGP – alpha acid glycoprotein.

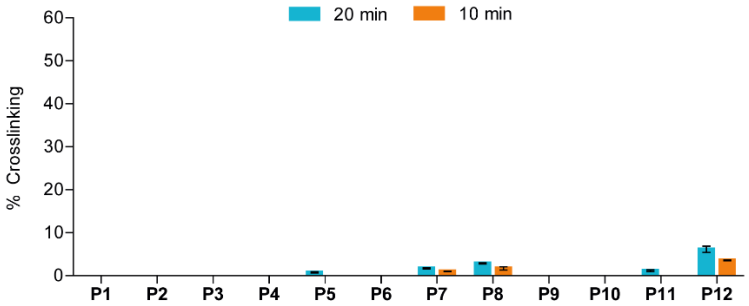

Figure S3: Crosslinking yields of probes **P1**-**P12** (2 µM) with recombinant CDK2 protein (1 µM) following irradiation with UV light (365 nm, 10 min and 20 min). Error bars indicate standard deviation over two replicates.

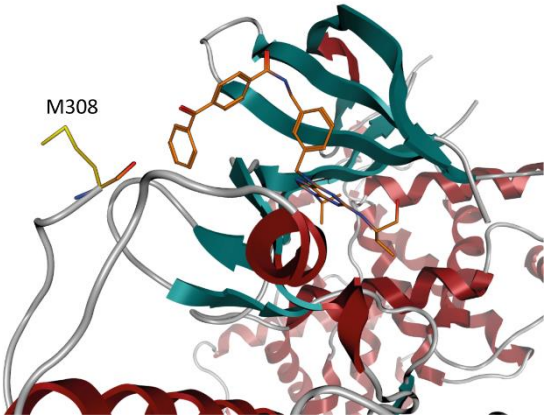

Figure S4: Modelled representation of **P9** bound to CDK9, based on the crystal structure of CDK9 with a roscovitine analogue (PBDID: 3LQ5), highlighting the proximity of the benzophenone to M308.

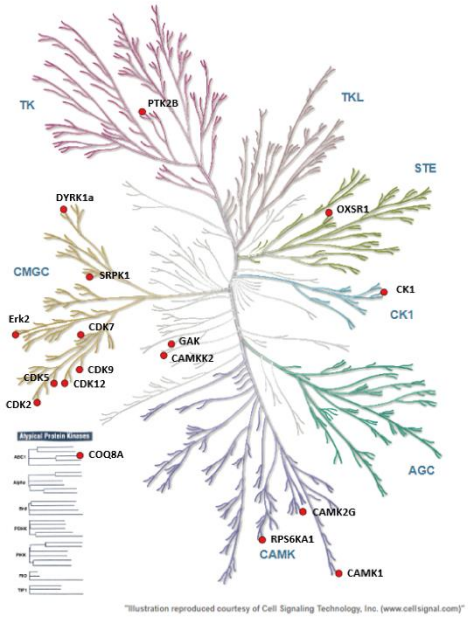

Figure S5: Kinome map highlighting the 17 kinases that were selectively enriched by **P12** from HL-60 cell lysates.

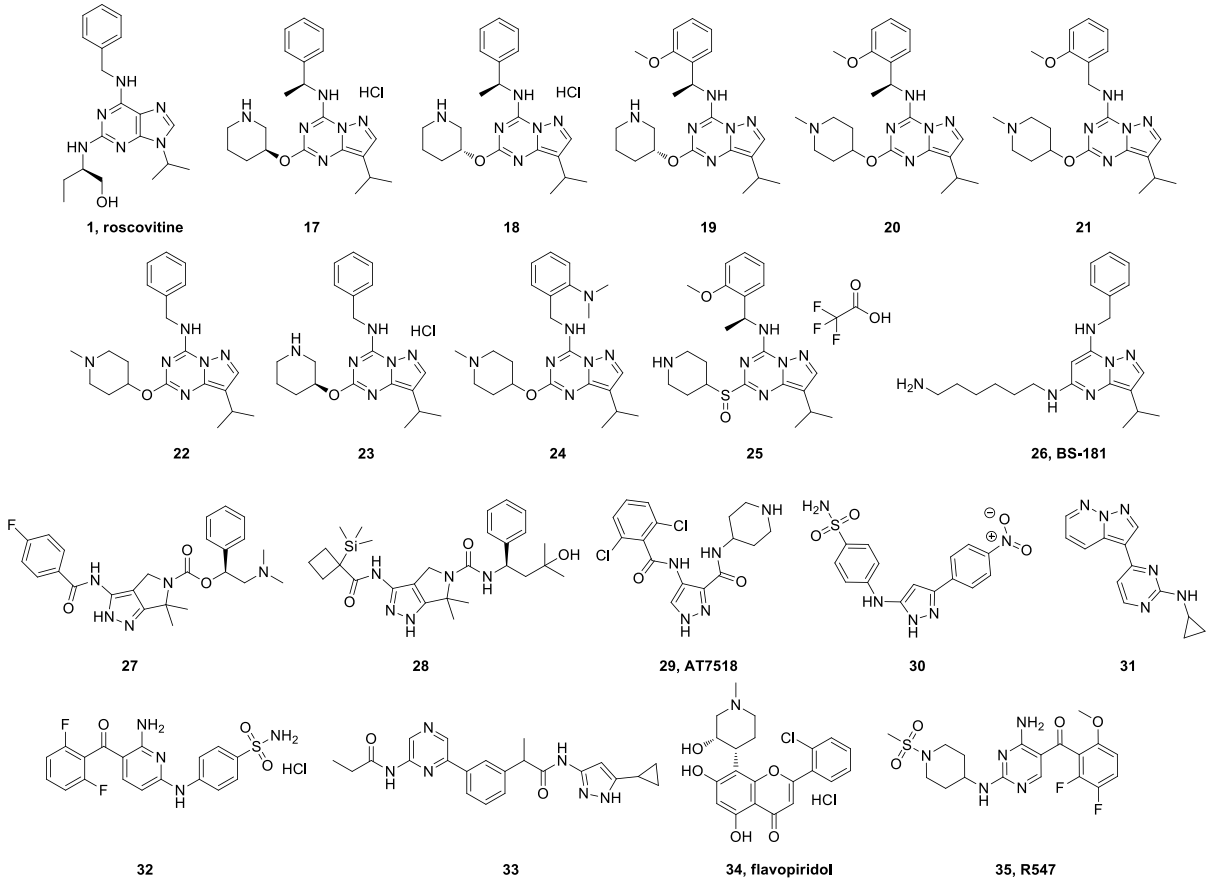

Figure S6: Structures of the 20 CDK inhibitors used for validation of the PhAST displacement assay to measure CDK2 binding, using **P12** as the reporter.

2. Synthetic chemistry

2.1 General experimental

Solvents were anhydrous and reagents purchased from commercial suppliers were used as received unless otherwise indicated.

2.1.1 Nuclear magnetic resonance (NMR) spectroscopy

Nuclear Magnetic Resonance spectra were recorded at ambient temperature using standard pulse methods on a Bruker AV-400 (^{1}H = 400 MHz, ^{13}C = 101 MHz, ^{18}F = 376 MHz) in the stated deuterated solvent and referenced either to residual undeuterated solvent or 0.03% (*v/v*) trimethylsilane (TMS).

2.1.2 Liquid chromatography-mass spectrometry (LC-MS) for small molecules

Liquid chromatography-mass spectrometry was carried out on an Aquity UPLC CSH C-18 column (internal diameter: 50 mm × 2.1 mm, packing diameter: 1.7 µm) at 40 °C with a 0.5 µL injection volume. The UV detection was a summed signal from wavelengths between 210 nm and 350 nm. Mass detection was performed with Alternate-scan Positive and Negative Electrospray on a Waters ZQ instrument, with a scan range of 100–1000 Da or 100–1200 Da (high mass range method). Scan time was 0.27 s with an inter-scan delay of 0.10 s.

2.1.2.1 LC-MS with an acidic modifier (Method A – [CSH~2min_For])

Sample was eluted using a gradient shown in **SI Table 1** with a flow rate of 1.0 mL/min.

- 0.1% *v/v* solution of formic acid in water (solvent A) and 0.1% *v/v* solution of formic acid in acetonitrile (solvent B).

SI Table 1: Low pH gradient for LC-MS analysis

Time (min)	A (%)	B (%)
0	97	3
1.5	5	95
1.9	5	95
2.0	97	3

2.1.2.2 LC-MS with a basic modifier (Method B – [CSH~2min_HPH])

Sample was eluted using a gradient shown in **SI Table 2** with a flow rate of 1.0 mL/min.

- 0.1% *v/v* 10 mM ammonium bicarbonate in water adjusted to pH 10 with ammonia solution (solvent A) and 0.1% *v/v* ammonia in acetonitrile (solvent B).

SI Table 2: High pH gradient for LC-MS analysis

Time (min)	A (%)	B (%)
0.00	97	3
0.05	97	3
1.5	5	95
1.9	5	95
2.00	97	3

2.1.3 High resolution mass spectrometry (HRMS)

High-resolution mass spectra were recorded on a Micromass Q-ToF Ulitma hybrid quadrupole time-of-flight mass spectrometer, with analytes separated on an Agilent 1100 Liquid Chromatography equipped with a Phenomenex luna C18 (2) reverse-phase column (100 mm × 2.1 mm, 3 µm packing diameter) at 35 °C. Samples were eluted using a gradient shown in **SI Table 3** with a flow rate of 0.5 mL/min. The injection volume was 2–5 µL. Mass to charge ratios (m/z) are reported in Daltons.

- 0.1% *v/v* solution of formic acid in water (solvent A) and 0.1% *v/v* solution of formic acid in acetonitrile (solvent B).

SI Table 3: Liquid chromatography conditions for high resolution mass spectrometry.

Time (min)	A (%)	B (%)
0.00	95	5
6.00	0	100
2.50	0	100
1.00	95	5
2.50	95	5

2.1.4 Mass directed automated preparative HPLC (MDAP)

Mass directed Autoprep (MDAP) was conducted on an Xselect CSH C18 column (internal diameter: 150mm x 30mm, packing diameter: 5µm) at ambient temperature. The solvents employed were 10mM ammonium bicarbonate adjusted to pH 10 with ammonia in water (solvent A) and acetonitrile (solvent B). The UV detection is a summed signal from wavelength of 210 nm to 350 nm. Mass spectra were recorded on a Waters ZQ mass spectrometer using alternate-scan positive and negative electrospray ionization. Mass detection was over the range 150–1000 Da. The scan time was 0.5 s with an inter-scan delay of 0.2 s. The following elution gradient was used as an example (High pH modifier, HpH):

SI Table 4: MDAP conditions for a high pH modifier

Time (min)	Flow rate (mL / min)	% A	% B
0	40	70	30
1	40	70	30
20	40	15	85
20.5	40	1	99
25	40	1	99

The gradient of acetonitrile required to elute product was determined by the LC-MS retention time. The following methods were selected dependent on the retention time of desired material:

SI Table 5: MDAP methods

Method	Flow rate (mL / min)	% B to % B	LCMS t_R (min)
A	40	0–25	0.40–0.65
B	40	15–55	0.65–0.90
C	40	30–85	0.90–1.16
D	40	50–99	1.16–1.40
E	40	80–99	1.40–2.00

2.1.5 Infrared spectroscopy

Infrared spectra were obtained on a Perkin Elmer Spectrum 100 FT-IR spectrometer with an ATR sampling accessory directly from a solid sample.

2.1.6 Melting point

All melting points were recorded on a Stuart SMP40 melting point apparatus and are uncorrected.

2.2 Synthetic schemes

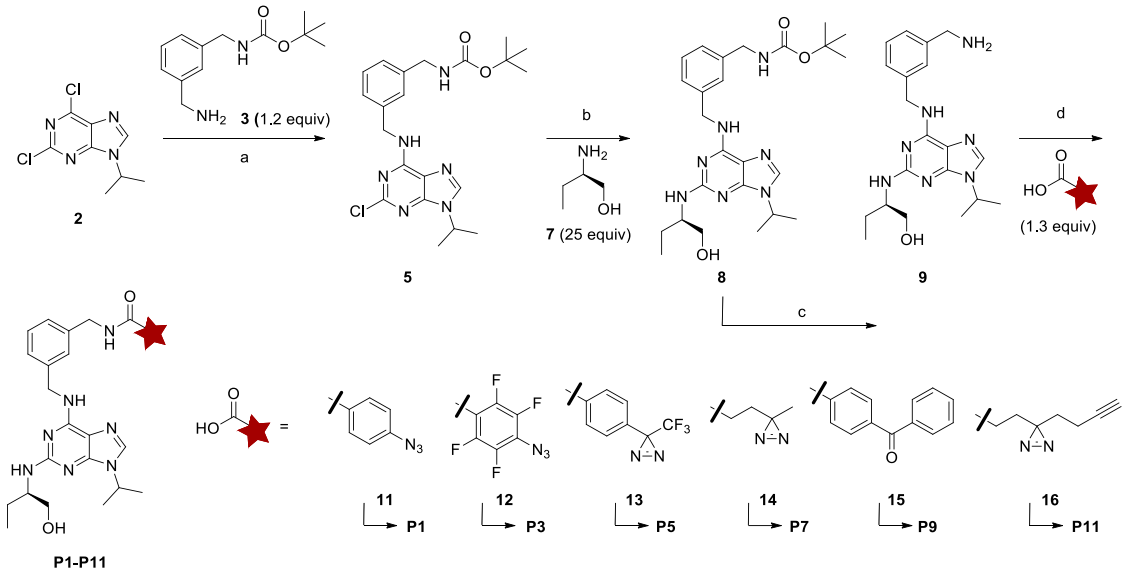

SI Scheme 1: Synthesis of *meta* substituted roscovitine derived photoaffinity probes. Reagents and conditions: a) TEA (1.6 equiv), 1-butanol, 100°C, 1 h, quantitative. b) 130°C, 60 h, **8** = 17%, **9** = 14%. c) TFA (20 equiv), CH_2Cl_2, 2 h, **9** = 87%. d) HATU (1.25 equiv), DIPEA (4 equiv), DMF, rt, 16 h, **P1** = 22%, **P3** = 40%, **P5** = 47%, **P7** = 34%, **P9** = 58% and **P11** = 72%.

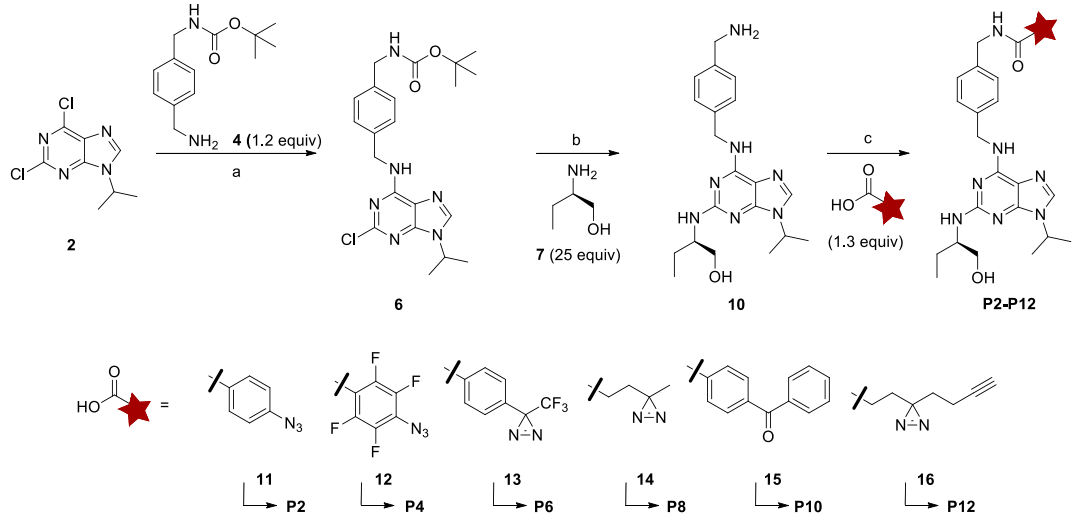

SI Scheme 2: Synthesis of *para* substituted roscovitine derived photoaffinity probes. Reagents and conditions: a) TEA (1.6 equiv), 1-butanol, 100°C, 1 h, quantitative. b) 130°C, 60 h, **10** = 94%. c) HATU (1.25 equiv), DIPEA (4 equiv), DMF, rt, 16 h, **P2** = 21%, **P4** = 17%, **P6** = 13%, **P8** = 34%, **P10** = 21% and **P12** = 15%.

2.3 Synthesis of intermediates

***Tert*-butyl 3-(((2-chloro-9-isopropyl-9*H*-purin-6-yl)amino)methyl)benzylcarbamate (5)**

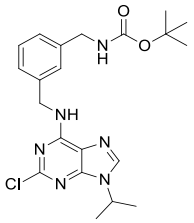

To a solution of 2,6-dichloro-9-isopropyl-9*H*-purine (**2**) (500 mg, 2.16 mmol) in 1-butanol (5 mL) in a microwave vial was added *tert*-butyl (3-(aminomethyl)benzyl)carbamate (**2**) (614 mg, 2.60 mmol). Triethylamine (0.48 mL, 3.46 mmol) was added and the microwave vial was sealed and heated thermally to 100 °C for 1 hour. The reaction mixture was concentrated to dryness and re-dissolved in ethyl acetate (10 mL). The solution was washed with water (10 mL) and the aqueous layer extracted with ethyl acetate (3 × 10 mL). The organics were combined, filtered through an Isolute® phase separator and concentrated to dryness *in vacuo* to yield crude *tert*-butyl-(3-(((2-chloro-9-isopropyl-9*H*-purin-6-yl)amino)methyl) benzyl) carbamate (**5**) (932 mg, 2.16 mmol, quantitative yield) as a clear gum. The crude material was carried forward to the next step without further purification. δ_H (400 MHz, CHLOROFORM-*d*) 7.71 (1H, s), 7.31–7.22 (3H, m), 7.26–7.22 (1H, m), 4.87–4.81 (1H, m), 3.18–3.10 (4H, m), 1.64 (6H, d, *J*=6.8 Hz), 1.44 (9H, s); LC-MS (Method [CSH~2min_HPH]): t_R = 1.21 min, 70% by UV, [M+H$^+$] found: 431.4.

***Tert*-butyl-(*R*)-(3-(((2-((1-hydroxybutan-2-yl)amino)-9-isopropyl-9*H*-purin-6-yl)amino)methyl)benzyl)carbamate (8)** and **(*R*)-2-((6-((3-(aminomethyl)benzyl)amino)-9-isopropyl-9*H*-purin-2-yl)amino)butan-1-ol (9)**

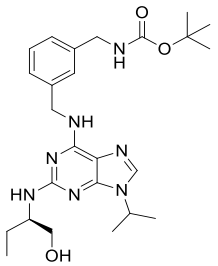

(**8**)

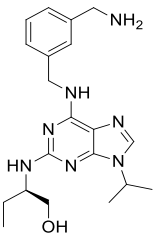

(**9**)

To crude *tert*-butyl-(3-(((2-chloro-9-isopropyl-9*H*-purin-6-yl)amino)methyl)benzyl) carbamate (**5**) (932 mg, 2.16 mmol) in a microwave vial was added (*R*)-2-aminobutan-1-ol (**7**) (5 mL, 53.1 mmol). The vial was placed under nitrogen and stirred thermally at 130 °C for 60 hours. Analysis by LC-MS indicated formation of a 1:1 mix of desired product and BOC-deprotected product. The reaction mixture was diluted with water and extracted with ethyl acetate (3 × 50 mL). The organics were combined, dried by filtration through an Isolute® phase separator and concentrated to dryness *in vacuo*. The reaction mixture was re-dissolved in methanol and loaded under gravity on to an Isolute® SCX-2, pre-wetted in methanol. The column was eluted with methanol to obtain the BOC-protected material (**8**). The column was then eluted with 2 M ammonia in methanol solution to obtain the BOC-deprotected material (**9**).

***Tert*-butyl-(*R*)-(3-(((2-((1-hydroxybutan-2-yl)amino)-9-isopropyl-9*H*-purin-6-yl)amino) methyl)benzyl)carbamate (8)**

The methanol solution containing (**8**) was concentrated to dryness *in vacuo* and added to a silica gel column (24 g) in a minimal amount of dichloromethane. The column was eluted with 20–30% 3:1 ethyl acetate:ethanol (1% triethylamine) in cyclohexane. The appropriate fractions were combined and concentrated to dryness *in vacuo* to yield the crude product which was contaminated with impurities. The residue was dissolved in methanol (1 mL) and purified by mass directed AutoPrep (Method C). The appropriate fractions were combined and concentrated to dryness *in vacuo* to afford *tert*-butyl-(*R*)-(3-(((2-((1-hydroxybutan-2-yl)amino)-9-isopropyl-9*H*-purin-6-yl)amino)methyl) benzyl)carbamate (**8**) (180 mg, 0.371 mmol, 17% yield) as an off-white solid; mp 121 – 123 ºC; ν_{max} (neat)/cm^{-1}: 3332, 2792, 1692, 1597, 1484, 1365, 1246, 1162 1047, 786, 668; δ_H (400 MHz, CHLOROFORM-*d*) 7.48 (1H, s), 7.29–7.24 (3H, m), 7.20–7.15 (1H, m), 6.09 (1H, br s), 4.96 (1H, br s), 4.94–4.88 (1H, m), 4.78–4.74 (2H, m), 4.60 (1H, spt, *J*=6.8 Hz), 4.28 (2H, br d, *J*=5.4 Hz), 3.96–3.86 (1H, m), 3.81 (1H, dd, *J*=10.5, 2.7 Hz) 3.63 (1H, dd, *J*=10.6, 7.7 Hz), 1.69–1.57 (2H, m), 1.53 (6H, d, *J*=6.8 Hz), 1.45 (9H, s), 1.02 (3H, t, *J*=7.5 Hz); δ_C (101 MHz, CHLOROFORM-*d*) 160.0 (C), 155.9 (CO), 154.8 (C), 150.3 (C), 139.3 (2 × C), 134.5 (CH), 128.8 (CH), 126.8 (CH), 126.6 (CH), 126.5 (CH), 114.7 (C), 79.5 (C), 68.3 (CH_2), 56.3 (CH), 46.4 (CH), 44.6 (CH_2), 44.4 (CH_2), 28.4 (3 × CH_3), 25.0 (CH_2), 22.6 (2 × CH_3), 10.9 (CH_3); LC-MS (Method [CSH~2min_HPH]): t_R = 1.09 min, 100% by UV, [M+H$^+$] found: 484.5; HRMS: ($C_{25}H_{38}N_7O_3$) [M+H$^+$] requires: 484.2958, [M+H$^+$] found: 484.3035.

(*R*)-2-((6-((3-(aminomethyl)benzyl)amino)-9-isopropyl-9*H*-purin-2-yl)amino)butan-1-ol (9)

The basic solution containing (**9**) was concentrated to dryness *in vacuo*, dissolved in methanol (1 mL) and purified by mass directed AutoPrep (Method B). The appropriate fractions were combined and concentrated to dryness *in vacuo* to afford (*R*)-2-((6-((3-(aminomethyl)benzyl)amino)-9-isopropyl-9*H*-purin-2-yl)amino) butan-1-ol (**9**) (113 mg, 0.295 mmol, 14% yield) as an off-white solid; mp 114 – 116 ºC; v_{max} (neat)/cm^{-1}: 3271, 2873, 1595, 1486, 1246, 1152, 1052, 884, 738; δ_H (400 MHz, CHLOROFORM-*d*) 7.48 (1H, s), 7.31–7.26 (2H, m), 7.25–7.21 (1H, m), 7.21–7.17 (1H, m), 6.20 (1H, br s), 4.90–4.82 (1H, m), 4.79–4.73 (2H, m), 4.60 (1H, spt, *J*=6.8 Hz), 3.96–3.86 (1H, m), 3.83–3.75 (3H, m), 3.62 (1H, dd, *J*=10.5, 7.3 Hz), 1.72–1.55 (2H, m), 1.53 (6H, dd, *J*=6.7, 2.6 Hz), 1.03 (3H, t, *J*=7.5 Hz); δ_C (101 MHz, CHLOROFORM-*d*) 160.0 (C), 154.8 (C), 143.5 (C), 139.2 (2 x C), 134.5 (CH), 128.7 (CH), 126.5 (CH), 126.2 (CH), 126.1 (CH), 114.7 (C), 67.9 (CH_2), 56.2 (CH), 46.4 (CH), 46.3 (CH_2), 44.4 (CH_2), 25.0 (CH_2), 22.6 (CH_3), 22.5 (CH_3), 11.0 (CH_3); LC-MS (Method [CSH~2min_HPH]): t_R = 0.82 min, 100% by UV, [M+H$^+$] found: 384.5; HRMS: ($C_{20}H_{30}N_7O$) [M+H$^+$] requires: 384.2433, [M+H$^+$] found: 384.2509.

(*R*)-2-((6-((3-(aminomethyl)benzyl)amino)-9-isopropyl-9*H*-purin-2-yl)amino)butan-1-ol (9)

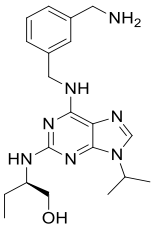

To a solution of *tert*-butyl-(*R*)-(3-(((2-((1-hydroxybutan-2-yl)amino)-9-isopropyl-9*H*-purin-6-yl)amino)methyl)benzyl)carbamate (**8**) (160 mg, 0.331 mmol) in dichloromethane (6.2 mL) was added trifluoroacetic acid (0.510 mL, 6.62 mmol) and the reaction was stirred at rt under nitrogen for two hours. The reaction mixture was concentrated to dryness *in vacuo.* The residue was re-dissolved in methanol and loaded under gravity on to an Isolute® SCX-2, pre-wetted in methanol. The column was eluted with methanol and then the product was eluted off the column with 2 M ammonia in methanol solution. The basic solution was concentrated to dryness *in vacuo* to afford (*R*)-2-((6-((3-(aminomethyl)benzyl)amino)-9-isopropyl-9*H*-purin-2-yl)amino)butan-1-ol (**9**) (111 mg, 0.289 mmol, 87% yield) as an off-white solid; spectral data consistent with above.

***Tert*-butyl-4-(((2-chloro-9-isopropyl-9*H*-purin-6-yl)amino)methyl)benzylcarbamate (6)**

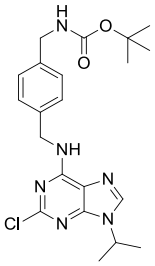

To a solution of 2,6-dichloro-9-isopropyl-9*H*-purine (**2**) (600 mg, 2.60 mmol) in 1-butanol (6 mL) in a microwave vial was added *tert*-butyl-(4-(aminomethyl)benzyl)carbamate (**4**) (736 mg, 3.12 mmol). Triethylamine (0.580 mL, 4.15 mmol) was added and the microwave vial was sealed and heated thermally to 100 °C for 1 hour. The reaction mixture was concentrated to dryness and re-dissolved in ethyl acetate (10 mL). The solution was washed with water (10 mL) and the aqueous layer extracted with ethyl acetate (3 × 10 mL). The organics were combined, dried through an Isolute® phase separator and concentrated to dryness *in vacuo* to yield crude *tert*-butyl-(4-(((2-chloro-9-isopropyl-9*H*-purin-6-yl)amino)methyl)benzyl)carbamate (**6**) (1194 mg, 2.77 mmol, quantitative yield) as a pale yellow solid; δ_H (400 MHz, CHLOROFORM-*d*) 7.68 (1H, br s), 7.35–7.30 (2H, m), 7.26–7.21 (2H, m), 6.54 (1H, br s), 4.94–4.88 (2H, m), 4.80 (1H, spt, *J*=6.8 Hz), 4.29 (2H, br d, *J*=5.4 Hz), 1.56 (6H, d, *J*=6.8 Hz), 1.46 (9H, s); LC-MS (Method [CSH~2min_HPH]): t_R = 1.21 min, 99% by UV, [M+H$^+$] found: 431.4.

(*R*)-2-((6-((4-(aminomethyl)benzyl)amino)-9-isopropyl-9*H*-purin-2-yl)amino)butan-1-ol (10)

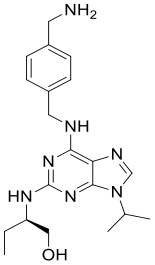

To *tert*-butyl (4-(((2-chloro-9-isopropyl-9*H*-purin-6-yl)amino)methyl)benzyl)carbamate (**6**) (1119 mg, 2.60 mmol) in a microwave vial was added (*R*)-2-aminobutan-1-ol (**7**) (5 mL, 53.1 mmol). The microwave vial was sealed and stirred at 130 °C for 60 hours. Analysis by LC-MS indicated formation

of the desired product and BOC-deprotection *in situ*. The reaction mixture was diluted with water and extracted with ethyl acetate (50 mL × 3). The organics were combined, dried through an Isolute® phase separator and concentrated *in vacuo*. The reaction mixture was purified by column chromatography (silica gel, 80g column), 50–75% (1% triethylamine) 3:1 ethyl acetate:ethanol in cyclohexane. The appropriate fractions were combined and concentrated to dryness *in vacuo* to afford (*R*)-2-((6-((4-(aminomethyl)benzyl)amino)-9-isopropyl-9*H*-purin-2-yl)amino)butan-1-ol (**10**) (938 mg, 2.446 mmol, 94% yield) as an off-white solid; mp 124 – 126 ºC; v_{max} (neat)/cm^{1} 3269, 2928, 1596, 1487, 1387, 1253, 1207, 1061, 787; δ_H ^{1}H NMR (400 MHz, CHLOROFORM-*d*) 7.45 (1H, s), 7.32–7.25 (2H, m), 7.24–7.18 (2H, m), 6.35 (1H, br s), 4.97–4.93 (1H, m), 4.71 (2H, m), 4.57 (1H, spt, *J*=6.8 Hz), 3.94–3.82 (1H, m), 3.82 (2H, s), 3.79 (1H, dd, *J*=10.8, 2.9 Hz), 3.61 (1H, dd, *J*=10.8, 7.3 Hz), 1.67–1.48 (8H, m), 1.00 (3H, t, *J*=7.6 Hz); δ_C ^{13}C NMR (101 MHz, CHLOROFORM-*d*) 1600 (C), 154.8 (C), 150.4 (C), 141.8 (C), 137.6 (C), 134.5 (CH), 127.9 (2 × CH), 127.3 (2 × CH), 114.6 (C), 67.8 (CH_2), 65.7 (CH_2), 56.1 (CH), 46.4 (CH), 46.0 (CH_2), 25.0 (CH_2), 22.5 (CH_3), 22.5 (CH_3), 10.9 (CH_3); LC-MS (Method [CSH~2min_HPH]): t_R = 0.81 min, 98% by UV, [M+H$^+$] found: 384.4; HRMS: ($C_{20}H_{30}N_7O$) [M+H$^+$] requires: 384.2504, [M+H$^+$] found: 384.2598.

2.4 Synthesis of probes

2.4.1 Commercially available photoreactive carboxylic acids

SI Table 6: Photoreactive groups commercially available as carboxylic acids.

Compound	Structure	Supplier	Catalogue number	CAS No.
11	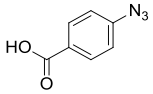	TCI	A0930	6427-66-3
12	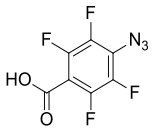	TCI	A2674	122590-77-6
13	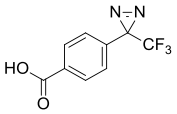	TCI	T2820	85559-46-2
14	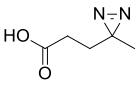	Enamine	EN300-97492	25055-86-1
15	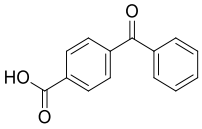	Sigma Aldrich	B12407	611-95-0
16	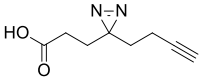	Enamine	EN300-702841	1450754-37-6

2.4.2 Synthesis of *meta* substituted roscovitine derived photoaffinity probes

(*R*)-4-azido-*N*-(3-(((2-((1-hydroxybutan-2-yl)amino)-9-isopropyl-9*H*-purin-6-yl)amino)methyl)benzyl)benzamide (P1)

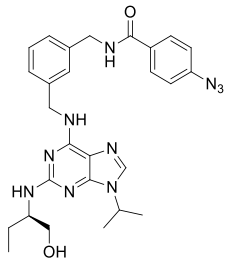

To a solution of 4-azidobenzoic acid (**11**) (17 mg, 0.102 mmol) **and** 1-[bis(dimethylamino) methylene]-1*H*-1,2,3-triazolo[4,5-*b*]pyridinium-3-oxide-hexafluorophosphate (37 mg, 0.098 mmol) in *N,N*-dimethylformamide (0.98 mL) was added diisopropylethylamine (0.07 mL, 0.375 mmol). The solution was stirred under nitrogen for 15 minutes before addition of (*R*)-2-((6-((3-(aminomethyl)benzyl)amino)-9-isopropyl-9*H*-purin-2-yl)amino)butan-1-ol (**9**) (30 mg, 0.078 mmol) and the reaction mixture stirred at rt overnight. The solution was directly purified by mass directed AutoPrep (Method C). The appropriate fractions were combined and concentrated to dryness *in vacuo* to afford (*R*)-4-azido-*N*-(3-(((2-((1-hydroxybutan-2-yl)amino)-9-isopropyl-9*H*-purin-6-yl)amino)methyl)benzyl)benzamide (**P1**) (9 mg, 0.017 mmol, 22% yield) as an off-white solid; mp 127 – 129 ºC; v_{max} (neat)/cm^{-1}: 3304, 2928, 2113, 1602, 1496, 1282, 848, 788; δ_H (400 MHz, CHLOROFORM-*d*) 7.82–7.77 (2H, m), 7.48 (1H, s),

7.31–7.22 (4H, m), 7.05–7.00 (2H, m), 6.86–6.75 (1H, m), 6.19 (1H, br s), 4.96–4.88 (1H, m), 4.72 (2H, br s), 4.65–4.51 (3H, m), 3.97–3.84 (1H, m), 3.77 (1H, dd, *J*=10.8, 2.9 Hz), 3.57 (1H, dd, *J*=10.8, 7.8 Hz), 1.67–1.50 (8H, m), 1.01 (3H, t, *J*=7.6 Hz); δ_C (101 MHz, CHLOROFORM-*d*) 166.5 (CO), 160.0 (C), 154.8 (C), 148.4 (C), 143.3 (C), 139.5 (C), 138.5 (C), 134.6 (CH), 130.9 (C), 129.0 (CH), 128.8 (2 × CH), 127.2 (CH), 127.1 (CH), 126.9 (CH), 118.9 (2 × CH), 114.7 (C), 68.3 (CH_2), 56.1 (CH), 46.4 (CH), 44.4 (CH_2), 44.1 (CH_2), 25.0 (CH_2), 22.6 (CH_3), 22.5 (CH_3), 10.9 (CH_3); LC-MS (Method [CSH~2min_HPH]): t_R = 1.08 min, 100% by UV, [M+H$^+$] found: 529.4; HRMS: ($C_{27}H_{33}N_{10}O_2$) [M+H$^+$] requires: 529.2710, [M+H$^+$] found: 529.2784.

(*R*)-4-azido-2,3,5,6-tetrafluoro-*N*-(3-(((2-((1-hydroxybutan-2-yl)amino)-9-isopropyl-9*H*-purin-6-yl)amino)methyl)benzyl)benzamide (P3)

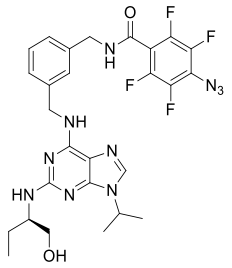

To a solution of 4-azido-2,3,5,6-tetrafluorobenzoic acid (**12**) (24 mg, 0.102 mmol) **and** 1-[bis(dimethylamino)methylene]-1*H*-1,2,3-triazolo[4,5-*b*]pyridinium-3-oxide-hexafluorophosphate (37 mg, 0.098 mmol) in *N,N*-dimethylformamide (0.98 mL) was added diisopropylethylamine (0.07 mL, 0.375 mmol). The solution was stirred under nitrogen for 15 minutes before addition of (*R*)-2-((6-((3-(aminomethyl)benzyl)amino)-9-isopropyl-9*H*-purin-2-yl)amino)butan-1-ol (**9**) (30 mg, 0.078 mmol) and the reaction mixture stirred at rt overnight. The reaction mixture was directly purified by mass directed AutoPrep (Method C). The appropriate fractions were combined and concentrated to dryness *in vacuo* to afford (*R*)-4-azido-2,3,5,6-tetrafluoro-*N*-(3-(((2-((1-hydroxybutan-2-yl)amino)-9-isopropyl-9*H*-purin-6-yl)amino)methyl)benzyl)benzamide (**P3**) (19 mg, 0.032 mmol, 40% yield) as an off-white solid; mp 122 – 124 ºC ν_{max} (neat)/cm^{-1}: 3283, 2928, 2126, 1652, 1487, 1389, 1263, 998, 788; δ_H (400 MHz, CHLOROFORM-*d*) 7.46 (1H, s), 7.31–7.20 (4H, m), 7.05 (1H, br s), 6.25 (1H, br s), 4.91–4.85 (1H, m), 4.71 (2H, br s), 4.63–4.51 (3H, m), 3.93–3.83 (1H, m), 3.72 (1H, dd, *J*=10.7, 2.7 Hz), 3.53–3.47 (1H, m), 1.65–1.46 (8H, m), 1.00 (3H, t, *J*=7.6 Hz); δ_C (101 MHz, CHLOROFORM-*d*) 160.0 (C), 157.6 (C), 154.7 (C), 139.6 (C), 137.3 (C), 134.6 (CH), 129.0 (CH), 127.0 (CH), 126.9 (CH), 126.8 (CH), 114.5 (C), 68.0 (CH_2), 56.0 (CH), 46.4 (CH), 44.2 (CH_2), 44.1 (CH_2), 24.9 (CH_2), 22.5 (CH_3), 22.4 (CH_3), 10.8 (CH_3); δ_F ^{19}F NMR (376 MHz, CHLOROFORM-*d*) -140.9 – -140.8 (2 F, m), -150.9 – -150.6 (2 F, m); LC-MS (Method [CSH~2min_HPH]): t_R = 1.14 min, 100% by UV, [M+H$^+$] found: 601.4; HRMS: ($C_{27}H_{29}F_4N_{10}O_2$) [M+H$^+$] requires: 601.2333, [M+H$^+$] found: 601.2414.

(*R*)-*N*-(3-(((2-((1-hydroxybutan-2-yl)amino)-9-isopropyl-9*H*-purin-6-yl)amino)methyl)benzyl)-4-(3-(trifluoromethyl)-3*H*-diazirin-3-yl)benzamide (P5)

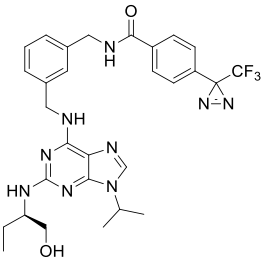

To a solution of 4-(3-(trifluoromethyl)-3*H*-diazirin-3-yl)benzoic acid (**13**) (18 mg, 0.078 mmol) and 1-[bis(dimethylamino)methylene]-1*H*-1,2,3-triazolo[4,5-*b*]pyridinium-3-oxide-hexafluorophosphate (37 mg, 0.098 mmol) in *N,N*-dimethylformamide (0.98 mL) was added diisopropylethylamine (0.07 mL, 0.375 mmol). The solution was stirred under nitrogen for 15 minutes before addition of (*R*)-2-((6-((3-(aminomethyl)benzyl)amino)-9-isopropyl-9*H*-purin-2-yl)amino)butan-1-ol (**9**) (30 mg, 0.078 mmol) and the reaction mixture stirred at rt overnight. The reaction mixture was directly purified by mass directed AutoPrep (Method D). The appropriate fractions were combined and concentrated to dryness *in vacuo* to afford (*R*)-*N*-(3-(((2-((1-hydroxybutan-2-yl)amino)-9-isopropyl-9*H*-purin-6-yl)amino)methyl)benzyl)-4-(3-(trifluoro methyl)-3*H*-diazirin-3-yl)benzamide (**P5**) (22 mg, 0.037 mmol, 47% yield) as an off-white solid; mp 121 – 123 ºC; ν_{max} (neat)/cm^{-1}: 1386, 2933, 1541, 1488, 1342, 1231, 1151, 940, 840, 741, 700; δ_H (400 MHz, CHLOROFORM-*d*) 7.86–7.78 (2H, m), 7.45 (1H, s), 7.26–7.15 (6H, m), 6.39 (1H, br s), 5.03–4.97 (1H, m), 4.67 (2H, br s), 4.61–4.46 (3H, m), 3.95–3.85 (1H, m), 3.74 (1H, dd, *J*=10.7, 2.7 Hz), 3.53 (1H, dd, *J*=10.8, 7.8 Hz), 1.69–1.46 (8H, m), 0.98 (3H, t, *J*=7.6 Hz); δ_C (101 MHz, CHLOROFORM-*d*) 166.2 (CO), 160.0 (C), 154.7 (C), 150.4 (C), 139.4 (C), 138.3 (C), 135.5 (C), 134.6 (CH), 132.2 (C), 128.9 (CH), 127.6 (2 × CH), 127.1 (CH), 127.0 (CH), 126.8 (CH), 126.5 (2 × CH), 123.3 (C), 120.5 (C), 114.6 (C), 68.1 (CH_2), 56.0 (CH), 46.4 (CH), 44.3 (CH_2), 44.1 (CH_2), 24.9 (CH_2), 22.6 (CH_3), 22.5 (CH_3), 10.9 (CH_3); δ_F ^{19}F NMR (376 MHz, CHLOROFORM-*d*) -65.1 (3 F, s); LC-MS (Method [CSH~2min_HPH]): t_R = 1.22 min, 100% by UV, [M+H$^+$] found: 596.4; HRMS: ($C_{29}H_{33}F_3N_9O_2$) [M+H$^+$] requires: 596.2631, [M+H$^+$] found: 596.2707.

(*R*)-*N*-(3-(((2-((1-hydroxybutan-2-yl)amino)-9-isopropyl-9*H*-purin-6-yl)amino)methyl)benzyl)-3-(3-methyl-3*H*-diazirin-3-yl)propanamide (P7)

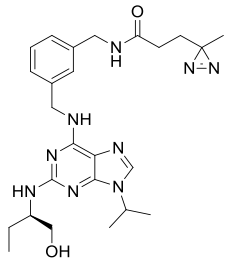

To a solution of 3-(3-methyl-3*H*-diazirin-3-yl)propanoic acid (**14**) (13 mg, 0.102 mmol) and 1-[bis(dimethylamino)methylene]-1*H*-1,2,3-triazolo[4,5-*b*]pyridinium-3-oxide-hexafluorophosphate **(**37 mg, 0.098 mmol) in *N*,*N*-dimethylformamide (0.98 mL) was added diisopropylethylamine (0.07 mL, 0.375 mmol). The solution was stirred under nitrogen for 15 minutes before addition of (*R*)-2-((6-((3-(aminomethyl)benzyl)amino)-9-isopropyl-9*H*-purin-2-yl)amino)butan-1-ol (30 mg, 0.078 mmol) (**9**) and the reaction mixture stirred at rt overnight. The reaction mixture was directly purified by mass directed AutoPrep (Method C). The appropriate fractions were combined and concentrated to dryness *in vacuo* to afford (*R*)-*N*-(3-(((2-((1-hydroxybutan-2-yl)amino)-9-isopropyl-9*H*-purin-6-yl)amino)methyl)benzyl)-3-(3-methyl-3*H*-diazirin-3-yl)propanamide (**P7**) (13 mg, 0.026 mmol, 34% yield) as an off-white solid; mp 113 – 115 ºC; ν_{max} (neat)/cm^{-1}: 3283, 2929, 1650, 1487, 1387, 1243, 1132, 1054, 884, 788, 701; δ_H (400 MHz, CHLOROFORM-*d*) 7.45 (1H, s), 7.26–7.17 (3H, m), 7.14–7.10 (1H, m), 6.39 (2H, br s), 5.02–4.96 (1H, m), 4.68 (2H, br s), 4.57 (1H, spt, *J*=6.8 Hz), 4.30 (2H, s), 3.95–3.86 (1H, m), 3.78 (1H, dd, *J*=10.8, 2.4 Hz), 3.58 (1H, dd, *J*=10.7, 7.6 Hz), 2.00–1.94 (2H, m), 1.76–1.69 (2H, m), 1.63–1.49 (8H, m), 1.03–0.96 (6H, m); δ_C (101 MHz, CHLOROFORM-*d*) 171.3 (CO), 160.0 (C), 154.8 (C), 150.4 (C), 139.4 (C), 138.5 (C), 134.5 (CH), 128.8 (CH), 127.0 (CH), 126.8 (CH), 126.7 (CH), 114.5 (C), 67.9 (CH_2), 56.0 (CH), 46.4 (CH), 44.2 (CH_2), 43.5 (CH_2), 30.5 (CH_2), 30.0 (CH_2), 25.4 (C), 24.9 (CH_2), 22.6 (CH_3), 22.5 (CH_3), 19.9 (CH_3), 10.9 (CH_3); LC-MS (Method [CSH~2min_HPH]): t_R = 0.99 min, 100% by UV, [M+H$^+$] found: 494.4; HRMS: ($C_{25}H_{36}N_9O_2$) [M+H$^+$] requires: 494.2914, [M+H$^+$] found: 494.2990.

(*R*)-4-benzoyl-*N*-(3-(((2-((1-hydroxybutan-2-yl)amino)-9-isopropyl-9*H*-purin-6-yl)amino)methyl)benzyl)benzamide (P9)

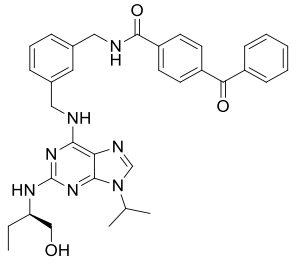

To a solution of 4-benzoylbenzoic acid (**15**) (18 mg, 0.078 mmol) and 1-[bis(dimethylamino) methylene]-1*H*-1,2,3-triazolo[4,5-*b*]pyridinium-3-oxide-hexafluorophosphate (37 mg, 0.098 mmol) in *N*,*N*-dimethylformamide (0.98 mL) was added diisopropylethylamine (0.07 mL, 0.375 mmol). The solution was stirred under nitrogen for 15 minutes before addition of (*R*)-2-((6-((3-(aminomethyl)benzyl)amino)-9-isopropyl-9*H*-purin-2-yl)amino)butan-1-ol (**9**) (30 mg, 0.078 mmol) and the reaction mixture stirred at rt overnight. The reaction mixture was directly purified by mass directed AutoPrep (Method C). The appropriate fractions were combined and concentrated to dryness *in vacuo* to afford (*R*)-4-benzoyl-*N*-(3-(((2-((1-hydroxybutan-2-yl)amino)-9-isopropyl-9*H*-purin-6-yl)amino)methyl)benzyl)benzamide (**P9**) (27 mg, 0.046 mmol, 58% yield) as an off-white solid; mp 131 – 133; ºC ν_{max} (neat)/cm^{-1}: 3299, 2923, 1598, 1487, 1275, 925, 787, 749, 699; δ_H (400 MHz, CHLOROFORM-*d*) 7.90 (2H, d, *J*=8.3 Hz), 7.81–7.73 (4H, m), 7.65–7.55 (1H, m), 7.52–7.41 (3H, m), 7.27–7.17 (4H, m), 6.40 (1H, br s), 5.03–4.98 (1H, m), 4.67 (2H, br s), 4.61–4.47 (3H, m), 3.95–3.83 (1H, m), 3.75 (1H, dd, *J*=10.8, 2.4 Hz), 3.55 (1H, dd, *J*=10.8, 7.8 Hz), 1.63–1.46 (8H, m), 0.98 (3H, t, *J*=7.6 Hz); δ_C (101 MHz, CHLOROFORM-*d*) 196.0 (CO), 166.5 (CO), 160.0 (C), 154.8 (C), 150.5 (C), 139.9 (C), 139.4 (C), 138.3 (C), 137.7 (C), 137.1 (C), 134.5 (CH), 132.8 (CH), 130.0 (2 × CH), 130.0 (2 × CH), 128.9 (CH), 128.4 (2 × CH), 127.1 (2 × CH), 127.1 (CH), 126.9 (CH), 126.8 (CH), 114.6 (C), 67.9 (CH_2), 56.0 (CH), 46.4 (CH), 44.2 (CH_2), 44.1 (CH_2), 24.9 (CH_2), 22.5 (CH_3), 22.5 (CH_3), 10.9 (CH_3); LC-MS (Method [CSH~2min_HPH]): t_R = 1.13 min, 100% by UV, [M+H$^+$] found: 592.4; HRMS: ($C_{34}H_{38}N_7O_3$) [M+H$^+$] requires: 592.2958, [M+H$^+$] found: 592.3036.

(*R*)-3-(3-(but-3-yn-1-yl)-3*H*-diazirin-3-yl)-*N*-(3-(((2-((1-hydroxybutan-2-yl)amino)-9-isopropyl-9*H*-purin-6-yl)amino)methyl)benzyl)

propanamide (P11)

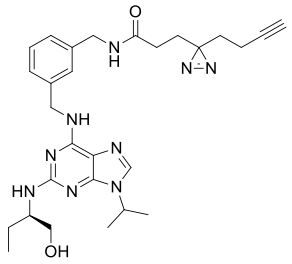

To a solution of 3-(3-(but-3-yn-1-yl)-3*H*-diazirin-3-yl)propanoic acid (**16**) (17 mg, 0.102 mmol) and 1-[bis(dimethylamino)methylene]-1*H*-1,2,3-triazolo[4,5-*b*]pyridinium-3-oxide-hexafluorophosphate (37 mg, 0.098 mmol) in *N,N*-dimethylformamide (0.98 mL) was added diisopropylethylamine (0.07 mL, 0.375 mmol). The solution was stirred under nitrogen for 15 minutes before addition of (*R*)-2-((6-((3-(aminomethyl)benzyl)amino)-9-isopropyl-9*H*-purin-2-yl)amino)butan-1-ol (**9**) (30 mg, 0.078 mmol) and the reaction mixture stirred at rt overnight. The reaction mixture was directly purified by mass directed AutoPrep (Method C). The appropriate fractions were combined and concentrated to dryness *in vacuo* to afford (*R*)-3-(3-(but-3-yn-1-yl)-3*H*-diazirin-3-yl)-*N*-(3-(((2-((1-hydroxybutan-2-yl)amino)-9-isopropyl-9*H*-purin-6-yl)amino)methyl)benzyl)propanamide (**P11**) (30 mg, 0.056 mmol, 72% yield) as an off-white solid; mp 108 – 110 ºC; ν_{max} (neat)/cm^{-1}: 3284, 2934, 1603, 1527, 1494, 1397, 1213, 1153, 980, 791; δ_H (400 MHz, CHLOROFORM-*d*) 7.48 (1H, s), 7.29–7.22 (3H, m), 7.18–7.13 (1H, m), 6.34–6.15 (2H, m), 4.97–4.93 (1H, m), 4.71 (2H, br s), 4.59 (1H, spt, *J*=6.8 Hz), 4.34 (2H, s), 3.96–3.87 (1H, m), 3.79 (1H, br d, *J*=10.3 Hz), 3.59 (1H, dd, *J*=10.5, 8.1 Hz), 2.01–1.93 (5H, m), 1.86–1.80 (2H, m), 1.66–1.54 (4H, m), 1.53 (6H, d, *J*=6.8 Hz), 1.02 (3H, t, *J*=8.3 Hz); δ_C (101 MHz, CHLOROFORM-*d*) 171.0 (CO), 160.0 (C), 154.8 (C), 150.4 (C), 139.4 (C), 138.4 (C), 134.6 (CH), 128.9 (CH), 127.1 (CH), 126.9 (CH), 126.8 (CH), 114.6 (C), 112.0 (C), 82.7 (C), 69.2 (CH), 68.2 (CH_2), 56.1 (CH), 46.4 (CH), 44.3 (CH_2), 43.7 (CH_2), 32.4 (CH_2), 30.2 (CH_2), 28.4 (CH_2), 25.0 (CH_2), 22.6 (CH_3), 22.5 (CH_3), 13.3 (CH_2), 10.9 (CH_3); LC-MS (Method [CSH~2min_HPH]): t_R = 1.04 min, 100% by UV, [M+H$^+$] found: 532.5; HRMS: ($C_{28}H_{38}N_9O_2$) [M+H$^+$] requires: 532.3070, [M+H$^+$] found: 532.3149.

2.4.2 Synthesis of *para* substituted roscovitine derived photoaffinity probes

(*R*)-4-azido-*N*-(4-(((2-((1-hydroxybutan-2-yl)amino)-9-isopropyl-9*H*-purin-6-yl)amino)methyl)benzyl)benzamide (P2)

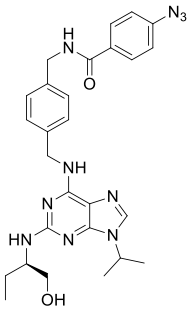

To a solution of 4-azidobenzoic acid (**11**) (83 mg, 0.508 mmol) and 1-[bis(dimethylamino)methylene]-1*H*-1,2,3-triazolo[4,5-*b*]pyridinium-3-oxide-hexafluorophosphate (186 mg, 0.489 mmol) in *N,N*-dimethylformamide (1.5 mL) was added diisopropylethylamine (0.33 mL, 1.877 mmol). The solution was stirred under nitrogen for 15 minutes before addition of (*R*)-2-((6-((4-(aminomethyl)benzyl)amino)-9-isopropyl-9*H*-purin-2-yl)amino)butan-1-ol (**10**) (150 mg, 0.391 mmol) and the reaction mixture stirred at rt overnight. The reaction mixture was directly purified by mass directed AutoPrep (Method C). The appropriate fractions were combined and concentrated to dryness *in vacuo* to afford (*R*)-4-azido-*N*-(4-(((2-((1-hydroxybutan-2-yl)amino)-9-isopropyl-9*H*-purin-6-yl)amino)methyl)benzyl)benzamide (**P2**) (43 mg, 0.081 mmol, 21% yield) as an off-white solid; mp 131 – 133 ºC; ν_{max} (neat)/cm^{-1}: 3299, 2931, 2114, 1599, 1488, 1388, 1214, 1151, 1051, 990, 846, 751, 665; δ_H (400 MHz, CHLOROFORM-*d*) 7.85–7.78 (2H, m), 7.43 (1H, s), 7.19–7.07 (4H, m), 7.02–6.96 (2H, m), 6.46 (1H, br s), 5.09 (1H, br s), 4.99–4.93 (1H, m), 4.79–4.45 (5H, m), 3.94–3.85 (1H, m), 3.76 (1H, br dd, *J*=10.5, 2.2 Hz), 3.56 (1H, dd, *J*=10.5, 7.6 Hz), 1.65–1.4 (8H, m), 0.99 (3H, t, *J*=7.6 Hz); δ_C (101 MHz, CHLOROFORM-*d*) 166.3 (C), 160.0 (CO), 154.8 (C), 150.3 (C), 143.2 (C), 138.2 (C), 137.2 (C), 134.5 (CH), 130.8 (C), 128.9 (2 × CH), 128.0 (2 × CH), 127.8 (2 × CH), 118.9 (2 × CH), 114.6 (C), 68.0 (CH_2), 56.0 (CH), 46.4 (CH), 44.0 (CH_2), 43.8 (CH_2), 24.9 (CH_2), 22.5 (CH_3), 22.4 (CH_3), 10.9 (CH_3); LC-MS (Method [CSH~2min_HPH]): t_R = 1.07 min, 100% by UV, [M+H$^+$] found: 529.4; HRMS: ($C_{27}H_{33}N_{10}O_2$) [M+H$^+$] requires: 529.2710, [M+H$^+$] found: 529.2788.

(*R*)-4-azido-2,3,5,6-tetrafluoro-*N*-(4-(((2-((1-hydroxybutan-2-yl)amino)-9-isopropyl-9*H*-purin-6-yl)amino)methyl)benzyl)benzamide (P4)

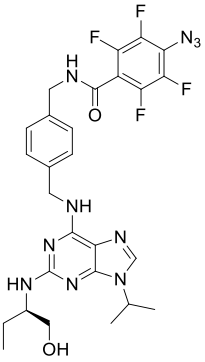

To a solution of 4-azido-2,3,5,6-tetrafluorobenzoic acid (**12**) (17 mg, 0.074 mmol) and 1-[bis(dimethylamino)methylene]-1*H*-1,2,3-triazolo[4,5-*b*]pyridinium-3-oxide-hexafluorophosphate (37 mg, 0.098 mmol) in *N,N*-dimethylformamide (1.5 mL) was added diisopropylethylamine (0.07 mL, 0.375 mmol). The solution was stirred under nitrogen for 15 minutes before addition of (*R*)-2-((6-((4-(aminomethyl)benzyl)amino)-9-isopropyl-9*H*-purin-2-yl)amino)butan-1-ol (**10**) (30 mg, 0.078 mmol) and the reaction mixture stirred at rt for 30 mins. The reaction mixture was directly purified by mass directed AutoPrep (Method C). The appropriate fractions were combined and concentrated to dryness *in vacuo* to afford (R)-4-azido-2,3,5,6-tetrafluoro-*N*-(4-(((2-((1-hydroxybutan-2-yl)amino)-9-isopropyl-9*H*-purin-6-yl)amino)methyl)benzyl)benzamide (**P4**) (8 mg, 0.013 mmol, 17% yield) as a white solid; mp 129 – 131 ºC; ν_{max} (neat)/cm^{-1}:2935, 2127, 1678, 1481, 1262, 996, 788; δ_H (400 MHz, CHLOROFORM-*d*) 7.46 (1H, s), 7.22 (4H, s), 7.10 (1H, br s), 6.31 (1H, br s), 4.93–4.88 (1H, m), 4.78–4.72 (1H, m), 4.65–4.49 (4H, m), 3.91–3.81 (1H, m), 3.74 (1H, dd, *J*=10.5, 2.8 Hz), 3.54 (1H, dd, *J*=10.7, 7.6 Hz), 1.63–1.53 (2H, m), 1.50 (6H, dd, *J*=6.8, 1.5 Hz), 1.01 (3H, t, *J*=7.5 Hz); δ_C (101 MHz, CHLOROFORM-*d*) 160.0 (C), 157.6 (C), 154.7 (C), 138.5 (C), 136.0 (C), 134.5 (CH), 127.9 (2 × CH), 127.9 (2 × CH), 114.6 (C), 68.3 (CH_2), 56.1 (CH), 46.5 (CH), 43.9 (2 × CH_2), 24.9 (CH_2), 22.5 (CH_3), 22.4 (CH_3), 10.9 (CH_3); δ_F (376 MHz, CHLOROFORM-*d*) -140.81 – -141.03 (2 F, m), -150.60 – -150.73 (2 F, m); LC-MS (Method [CSH~2min_HPH]): t_R = 1.13 min, 95% by UV, [M+H$^+$] found: 601.4; HRMS: ($C_{27}H_{29}F_4N_{10}O_2$) [M+H$^+$] requires: 601.2333, [M+H$^+$] found: 601.2411.

(*R*)-*N*-(4-(((2-((1-hydroxybutan-2-yl)amino)-9-isopropyl-9*H*-purin-6-yl)amino)methyl)benzyl)-4-(3-(trifluoromethyl)-3*H*-diazirin-3-yl)benzamide (P6)

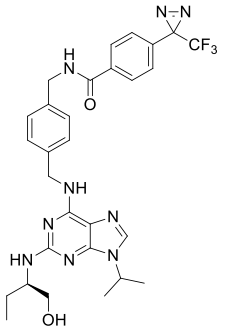

To a solution of 4-(3-(trifluoromethyl)-3*H*-diazirin-3-yl)benzoic acid (**13**) (117 mg, 0.508 mmol) **and** 1-[bis(dimethylamino)methylene]-1*H*-1,2,3-triazolo[4,5-*b*]pyridinium-3-oxide-hexafluorophosphate (186 mg, 0.489 mmol) in *N,N*-dimethylformamide (1.5 mL) was added diisopropylethylamine (0.33 mL, 1.877 mmol). The solution was stirred under nitrogen for 15 minutes before addition of (*R*)-2-((6-((4-(aminomethyl)benzyl)amino)-9-isopropyl-9*H*-purin-2-yl)amino)butan-1-ol (**10**) (150 mg, 0.391 mmol) and the reaction mixture stirred at rt overnight. The reaction mixture was directly purified by mass directed AutoPrep (Method D). The appropriate fractions were combined and concentrated to dryness *in vacuo* to afford (*R*)-*N*-(4-(((2-((1-hydroxybutan-2-yl)amino)-9-isopropyl-9*H*-purin-6-yl)amino)methyl)benzyl)-4-(3-(trifluoromethyl)-3*H*-diazirin-3-yl)benzamide (**P6**) (31 mg, 0.052 mmol, 13% yield) as an off-white solid; mp 127 – 129 ºC; ν_{max} (neat)/cm^{-1}: 3289, 2934, 1599, 1488, 1343, 1185, 1153, 939, 788, 741; δ_H (400 MHz, CHLOROFORM-*d*) 7.87–7.81 (2H, m), 7.45 (1H, s), 7.23–7.07 (6H, m), 6.38 (1H, br s), 4.96–4.90 (1H, m), 4.79–4.45 (5H, m), 3.94–3.83 (1H, m), 3.76 (1H, dd, *J*=10.5, 2.2 Hz), 3.56 (1H, dd, *J*=10.5, 7.6 Hz), 1.66–1.45 (8H, m), 1.00 (3H, t, *J*=7.6 Hz); δ_C (101 MHz, CHLOROFORM-*d*) 166.1 (CO), 160.0 (C), 154.8 (C), 150.3 (C), 138.3 (C), 136.9 (C), 135.5 (C), 134.5 (CH), 132.2 (C), 128.0 (2 × CH), 127.8 (2 × CH), 127.6 (2 × CH), 126.5 (2 × CH), 123.3 (C), 120.5 (C), 114.6 (C), 68.1 (CH_2), 56.1 (CH), 46.4 (CH), 44.0 (CH_2), 43.9 (CH_2), 24.9 (CH_2), 22.5 (CH_3), 22.4 (CH_3), 10.9 (CH_3); δ_C ^{19}F NMR (376 MHz, CHLOROFORM-*d*) -65.1 (3 F, s); LC-MS (Method [CSH~2min_HPH]): t_R = 1.21 min, 96% by UV, [M+H$^+$] found: 596.4; HRMS: ($C_{29}H_{33}F_3N_9O_2$) [M+H$^+$] requires: 596.2631, [M+H$^+$] found: 596.2709.

(*R*)-*N*-(4-(((2-((1-hydroxybutan-2-yl)amino)-9-isopropyl-9*H*-purin-6-yl)amino)methyl)benzyl)-3-(3-methyl-3*H*-diazirin-3-yl)propanamide (P8)

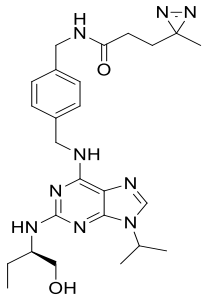

To a solution of 3-(3-methyl-3*H*-diazirin-3-yl)propanoic acid (**14**) (65 mg, 0.508 mmol) and 1-[bis(dimethylamino)methylene]-1*H*-1,2,3-triazolo[4,5-*b*]pyridinium-3-oxide-hexafluorophosphate (186 mg, 0.489 mmol) in *N,N*-dimethylformamide (1.5 mL) was added diisopropylethylamine (0.33 mL, 1.877 mmol). The solution was stirred under nitrogen for 15 minutes before addition of (*R*)-2-((6-((4-(aminomethyl)benzyl)amino)-9-isopropyl-9*H*-purin-2-yl)amino)butan-1-ol (**10**) (150 mg, 0.391 mmol) and the reaction mixture stirred at rt overnight. The reaction mixture was directly purified by mass directed AutoPrep (Method B). The appropriate fractions were combined and concentrated to dryness *in vacuo* to afford (*R*)-*N*-(4-(((2-((1-hydroxybutan-2-yl)amino)-9-isopropyl-9*H*-purin-6-yl)amino)methyl)benzyl)-3-(3-methyl-3*H*-diazirin-3-yl)propanamide (**P8**) (65 mg, 0.132 mmol, 34% yield) as an off-white solid; mp 116 – 118 ºC; ν_{max} (neat)/cm^{-1}: 3287, 2930, 1648, 1512, 1417, 1353, 1244, 1133, 1051, 910, 884, 751, 664; δ_H (400 MHz, CHLOROFORM-*d*) 7.42 (1H, s), 7.20–7.14 (2H, m), 7.12–7.07 (2H, m), 6.69–6.46 (2H, m), 5.05–4.99 (1H, m), 4.76–4.48 (3H, m), 4.36–4.28 (2H, m), 3.91–3.81 (1H, m), 3.74 (1H, dd, *J*=10.5, 2.8 Hz), 3.56 (1H, dd, *J*=10.7, 7.4 Hz), 1.99–1.93 (2H, m), 1.75–1.69 (2H, m), 1.62–1.45 (8H, m), 1.00–0.94 (6H, m); δ_C (101 MHz, CHLOROFORM-*d*) 171.3 (CO), 160.0 (C), 154.8 (C), 150.3 (C), 138.2 (C), 137.1 (C), 134.4 (CH), 127.9 (2 × CH), 127.7 (2 × CH), 114.5 (C), 67.7 (CH_2), 55.9 (CH), 50.2 (C), 46.4 (CH), 43.9 (CH_2), 43.3 (CH_2), 30.4 (CH_2), 30.0 (CH_2), 24.9 (CH_2), 22.5 (CH_3), 22.4 (CH_3), 19.9 (CH_3), 10.9 (CH_3); LC-MS (Method [CSH~2min_HPH]): t_R = 0.69 min, 94% by UV, [M+H$^+$] found: 494.4; HRMS: ($C_{25}H_{36}N_9O_2$) [M+H$^+$] requires: 494.2914, [M+H$^+$] found: 494.2990.

(*R*)-4-benzoyl-*N*-(4-(((2-((1-hydroxybutan-2-yl)amino)-9-isopropyl-9*H*-purin-6-yl)amino)methyl)benzyl)benzamide (P10)

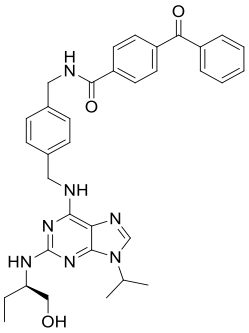

To a solution of 4-benzoylbenzoic acid (**15**) (115 mg, 0.508 mmol) and 1-[bis(dimethylamino)methylene]-1*H*-1,2,3-triazolo[4,5-*b*]pyridinium-3-oxide-hexafluorophosphate (186 mg, 0.489 mmol) in *N,N*-dimethylformamide (1.5 mL) was added diisopropylethylamine (0.33 mL, 1.877 mmol). The solution was stirred under nitrogen for 15 minutes before addition of (*R*)-2-((6-((4-(aminomethyl)benzyl)amino)-9-isopropyl-9*H*-purin-2-yl)amino)butan-1-ol (**10**) (150 mg, 0.391 mmol) and the reaction mixture stirred at rt overnight. The reaction mixture was directly purified by mass directed AutoPrep (Method C). The appropriate fractions were combined and concentrated to dryness *in vacuo* to afford (*R*)-4-benzoyl-*N*-(4-(((2-((1-hydroxybutan-2-yl)amino)-9-isopropyl-9*H*-purin-6-yl)amino)methyl)benzyl)benzamide (**P10**) (48 mg, 0.081 mmol, 21% yield) as an off-white solid; mp 134 – 136 ºC ν_{max} (neat)/cm^{-1}: 3297, 2929, 1651, 1597, 1487, 1389, 1276, 1052, 925, 751, 656; δ_H (400 MHz, CHLOROFORM-*d*) 7.95–7.88 (2H, m), 7.80–7.73 (4H, m), 7.62–7.56 (1H, m), 7.50–7.42 (3H, m), 7.31–7.18 (4H, m), 6.46 (1H, br s), 4.99–4.95 (1H, m), 4.78–4.49 (5H, m), 3.93–3.83 (1H, m), 3.76 (1H, dd, *J*=10.7, 2.7 Hz), 3.56 (1H, dd, *J*=10.8, 7.5 Hz), 1.6–1.45 (8H, m), 0.98 (3H, t, *J*=7.6 Hz); δ_C (101 MHz, CHLOROFORM-*d*) 196.0 (CO), 166.5 (CO), 160.0 (C), 154.8 (C), 150.3 (C), 140.0 (C), 138.3 (C), 137.7 (C), 137.1 (C), 137.0 (C), 134.5 (CH), 132.8 (CH), 130.0 (2 × CH), 130.0 (2 × CH), 128.4 (2 × CH), 128.1 (2 × CH), 127.8 (2 × CH), 127.1 (2 × CH), 114.6 (C), 67.9 (CH_2), 56.0 (CH), 46.4 (CH), 44.0 (CH_2), 43.9 (CH_2), 24.9 (CH_2), 22.5 (CH_3), 22.4 (CH_3), 10.9 (CH_3); LC-MS (Method [CSH~2min_HPH]): t_R = 1.12 min, 97% by UV, [M+H$^+$] found: 592.4; HRMS: ($C_{34}H_{38}N_7O_3$) [M+H$^+$] requires: 592.2958, [M+H$^+$] found: 592.3035.

(*R*)-3-(3-(but-3-yn-1-yl)-*3H*-diazirin-3-yl)-*N*-(4-(((2-((1-hydroxybutan-2-yl)amino)-9-isopropyl-9*H*-purin-6-yl)amino)methyl)benzyl)

propanamide (P12)

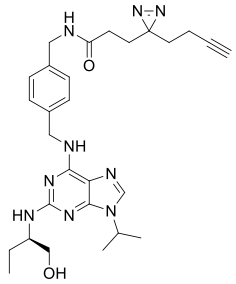

To a solution of 3-(3-(but-3-yn-1-yl)-3*H*-diazirin-3-yl)propanoic acid (**16**) (65 mg, 0.391 mmol) and 1-[bis(dimethylamino)methylene]-1*H*-1,2,3-triazolo[4,5-*b*]pyridinium-3-oxide-hexafluorophosphate (186 mg, 0.489 mmol) in *N,N*-dimethylformamide (1.5 mL) was added diisopropylethylamine (0.33 mL, 1.877 mmol). The solution was stirred under nitrogen for 15 minutes before addition of (*R*)-2-((6-((4-(aminomethyl)benzyl)amino)-9-isopropyl-9*H*-purin-2-yl)amino)butan-1-ol (**10**) (150 mg, 0.391 mmol) and the reaction mixture stirred at rt overnight. The reaction mixture was directly purified by mass directed AutoPrep (Method B). The appropriate fractions were combined and concentrated to dryness *in vacuo* to afford (*R*)-3-(3-(but-3-yn-1-yl)-3*H*-diazirin-3-yl)-*N*-(4-(((2-((1-hydroxybutan-2-yl)amino)-9-isopropyl-9*H*-purin-6-yl)amino)methyl)benzyl)propanamide (**P12**) (32 mg, 0.060 mmol, 15% yield) as an off-white solid; mp 117 – 119 ºC; ν_{max} (neat)/cm^{-1}: 3288, 2930, 1597, 1487, 1388, 1243, 1020, 788; δ_H (400 MHz, CHLOROFORM-*d*) 7.45 (1H, s), 7.24–7.19 (2H, m), 7.17–7.11 (2H, m), 6.43–6.22 (2H, m), 4.98–4.92 (1H, m), 4.79–4.50 (3H, m), 4.41–4.27 (2H, m), 3.93–3.83 (1H, m), 3.77 (1H, dd, *J*=10.5, 2.5 Hz), 3.58 (1H, dd, *J*=10.7, 7.7 Hz), 2.02–1.90 (5H, m), 1.86–1.79 (2H, m), 1.66–1.53 (4H, m), 1.50 (6H, dd, *J*=6.8, 1.0 Hz), 1.00 (3H, t, *J*=7.5 Hz); δ_C (101 MHz, CHLOROFORM-*d*) 171.0 (CO), 160.0 (C), 154.8 (C), 150.3 (C), 138.2 (C), 137.1 (C), 134.5 (CH), 128.0 (2 × CH), 127.8 (2 × CH), 114.6 (C), 82.7 (C), 69.2 (CH), 68.0 (CH_2), 56.1 (CH), 46.4 (CH), 44.0 (CH_2), 43.4 (CH_2), 32.4 (CH_2), 30.2 (CH_2), 28.4 (CH_2), 27.9 (C), 24.9 (CH_2), 22.6 (CH_3), 22.5 (CH_3), 13.3 (CH_2), 10.9 (CH_3); LC-MS (Method [CSH~2min_HPH]): t_R = 0.75 min, 93% by UV, [M+H$^+$] found:532.5; HRMS: ($C_{28}H_{38}N_9O_2$) [M+H$^+$] requires: 532.3070, [M+H$^+$] found: 532.3151.

3. Characterisation assays

3.1 CDK2, CDK7 and CDK9 ADP-Glo^{TM} assays

3.1.1 Protein source

CDK2 protein purchased under exclusive license from Dundee consortium: co-expressed GST-CDK2 with Cyclin A (DU43557).
CDK7 protein purchased under exclusive license from Dundee consortium: co-expressed CDK7 with MAT1 and Cyclin H (DU49574).
CDK9 protein purchased under exclusive license from Dundee consortium: co-expressed GST-CDK9 with Cyclin T1 (DU31050).

3.2.1 ADP-Glo^{TM} assay protocol

Proteins, either 0.03 µM CDK7/MAT1/Cyclin H, 0.03 µM CDK9/Cyclin T1 or 0.004 µM CDK2/Cyclin A (all from Dundee Consortium) were diluted in assay buffer (50 mM HEPES pH 7.4, 10 mM MgCl2, 1 mM CHAPS, 1 mM DTT) and preincubated for 30 mins with 11 point, 1 in 4 serial dilutions of test compounds dissolved in DMSO in Greiner white low volume plates (#784075). Reactions were initiated upon addition of 20 µM CDK7/9-tide (ThermoScientific PV5090) prepared in assay buffer containing either 30 µM ATP (CDK7/MAT1/Cyclin H) or 60 µM ATP (CDK9/Cyclin T1), or 20 µM CDK2-tide (GGGPATPKKAKKL) prepared in assay buffer containing 30 µM ATP (CDK2/Cyclin A) at a final assay volume of 6 µL and incubated at room temperature for 60 min. Reactions were subsequently quenched upon addition of 6 µL of ADP-Glo 1 reagent which was incubated for 60 min before addition of 12 µL of ADP-Glo 2 reagent and a final incubation of 40 min. The plates were read on a PHERAstar (signal stable for 30-90min following Glo 2 addition) and the data was processed using a standard XC50 4-parameter logistic curve fit algorithm in Activity Base.

SI Table 7: Instrument details

Instrument	Parameter	Condition
PHERAstar FS Plate reader (BMG Labtech)	Gain	3600
	Focal height	13.7 mm (top read)
	Measurement interval time	1.0 s
	Optic module	LUM plus
	Top read settling time	0.2 s
	Measurement start time	0 s

3.2 ChromLogD$_{7.4}$

Chromatographic hydrophobicity index (ChiLogD7.4) was determined by fast-gradient HPLC, according to literature procedures,[1] using a Waters Aquity UPLC System, Phenomenex Gemini NX 50 × 2 mm, 3 µm HPLC column, 0−100% pH 7.40 ammonium acetate buffer/acetonitrile gradient. Retention time was compared to standards of known pH to derive the Chromatographic Hydrophobicity Index (CHI). ChromLogD = 0.0857CHI − 2.

3.3 Human serum albumin binding (%)

Percentage binding to human serum albumin was measured using the published protocol.[2]

3.4 Alpha acid glycoprotein binding (%)

Percentage binding to alpha acid glycoprotein was measured using the published protocol.[3]

3.5 Solubility

Compounds to be tested (10 mM, 5 µL in DMSO) were diluted to 100 µL in PBS (pH 7.4), equilibrated for 1 hour at room temperature and filtered through Millipore Multiscreen$_{HTS}$-PCF filter plates (MSSL BPC). The filtrate was quantified using a suitably calibrated Charged Aerosol Detector.[4]

3.6 Artificial membrane permeability

Permeability across a lipid membrane was measured using the published protocol.[5]

4. Photocrosslinking experiments with CDK2, CDK7 and CDK9 recombinant protein

4.1 General experimental

Irradiation was carried out using a CL-1000 Ultraviolet Crosslinker at 302 nm or 365 nm.

Intact protein masses were recorded by liquid chromatography-mass spectrometry (LC-MS) using a 6224 ToF (Agilent) Accurate Mass Series mass spectrometer, interfaced with an Agilent 1200 liquid chromatography and sample handling system. The protein sample was injected using an Agilent 1200 series AutoSampler (Model No. G1367B) with a 10 µL injection volume and maintained at a temperature of 10 °C. Chromatography was carried out on an Agilent Bio-HPLC PLRP-S (1000Å, 5 µm × 50 mm × 1.0 mm, PL1312-1502) reverse phase HPLC column at 70 °C. Using an Agilent 1200 series binary pump system (Model No. G1312B) the sample was eluted at 0.5 mL/min using a gradient system from Solvent A (water, 0.2 % (*v/v*) formic acid) to Solvent B (acetonitrile, 0.2 % (*v/v*) formic acid) according to the following conditions:

SI Table 8: Elution gradient (%B) used for intact protein LC-MS

Time	%B	Flow	Pressure
0	10	0.5 ml/min	350
0.5	30	0.5 ml/min	350
5.00	58	0.5 ml/min	350
5.70	65	0.5 ml/min	350
5.71	100	0.5 ml/min	350
6.20	100	0.5 ml/min	350
6.21	10	0.5 ml/min	350
8.00	10	0.5 ml/min	350
8.10	10	0.5 ml/min	350

The eluent was injected directly into an Agilent ToF mass spectrometer (Model No. G6224A) using a dual ESI source and scanning between 600-3200 Da with a scan rate of 1.03 s in positive mode. The following MS parameters were used: Capillary voltage limit – 4200; Desolvation temperature – 340 ºC; Drying gas flow – 8.0 l/min. Data acquisition was carried out in 2 GHz Extended Dynamic range mode. Spectra were processed using Mass Hunter Qualitative Analysis™ B06.00 (Agilent) software with the Maximum Entropy method employed. The total ion chromatograms (TIC) were extracted (region containing protein) and the summed scans were deconvoluted over a m/z range with an expected mass range dependent on the protein (see **SI Table 9**). The peak areas for unmodified protein and labelled protein were recorded and used to calculate % photocrosslinking using the equation:

% = ((crosslinked protein)/(protein only+(crosslinked protein)))*100

SI Table 9: Deconvolution conditions

Expected mass range	m/z range	Expected mass range

CDK2 (1st construct) Used in crosslinking yield comparison of probes	700-2000	30000-40000
CDK2 (2nd construct) Used in displacement assay + site of crosslinking	850-2200	36000-40000
CDK7	650-1100	37000-43000
CDK9	850-1600	65000-75000

4.2 Study of percentage photocrosslinking of probes **P1-P12** with CDK2, CDK7 and CDK9

Preparation of protein stock solutions:
CDK2 (co-expressed cyclin-A1) (25 µL, 18.7 µM) was thawed at 0 ºC and 385 µL of buffer was added to give 460 µL of 1 µM stock solution.
CDK7-His (co-expressed cyclin-H+MAT1) (50 µL, 8 µM) was thawed at 0 ºC and 350 µL of buffer was added to give 400 µL of 1 µM stock solution
CDK9-GST (co-expressed cyclin-T1) (47 µL, 8.5 µM) was thawed at 0 ºC and 353 µL of buffer was added to give 400 µL of 1 µM stock solution.
Buffer = 50 mM HEPES, 10 mM $MgCl_2$.

Example procedure: 150 nL of photoaffinity probe **X** (200 µM in DMSO) was transferred into a Greiner 384 low volume plate (#784076) using a Labcyte Echo 555 Liquid Handler®. 15 µL protein stock solution (1 µM) was added to the well containing probe **X** and incubated at 4 °C on ice for 15 min (Final probe concentration = 2 µM). The plate was irradiated at 302 nm for 10 min on ice. The plate was sealed, centrifuged (1000 rpm, 1 min) and sampled directly for intact protein LC-MS analysis using the methods described in SI Section 4.1. This experiment was performed for all 12 probes (**P1-P12**) against CDK2, CDK7 and CDK9 recombinant protein in duplicate.

4.2.1 Data tables of photocrosslinking yields for probes **P1-P12** against CDK2, CDK7 and CDK9 recombinant protein

SI Table 10: Crosslinking yields of probe **P1-P12** against CDK2, CDK7 and CDK9

	CDK2		**CDK7**		**CDK9**	
Probe	**Mean**	**SD**	**Mean**	**SD**	**Mean**	**SD**
P1	9.09	0.27	31.58	8.25	29.71	1.71
P3	22.53	3.81	32.77	7.93	31.00	1.03
P5	1.12	0.35	0.00	0.00	7.76	0.47
P7	9.64	2.36	34.56	0.45	26.77	0.58
P9	0.00	0.00	5.90	8.34	40.53	1.69
P2	16.89	12.89	29.54	1.88	31.54	3.23
P4	17.36	2.52	29.74	0.98	38.42	0.16
P6	0.00	0.00	0.00	0.00	6.60	0.32
P8	10.15	0.17	35.03	2.84	22.68	1.99
P10	1.17	0.06	0.00	0.00	53.12	1.71
P11	12.25	0.27	23.75	1.92	16.18	4.54
P12	14.80	0.03	41.43	1.01	34.02	0.75

4.3 Study of percentage photocrosslinking of probes **P1**-**P12** with CDK2 at 365 nm

Preparation of protein stock solutions:
CDK2 protein provided under Genescript/GSK collaboration: 6H-Flag-Tev-CDK2 (41 µM).
CDK2 (20 µL, 41 µM) was thawed at 0 ºC and 780 µL of buffer was added to give 800 µL of 1 µM stock solution

Example procedure: 150 nL of photoaffinity probe **X** (200 µM in DMSO) was transferred into a Greiner 384 low volume plate (#784076) using a Labcyte Echo 555 Liquid Handler®. 15 µL protein stock solution (1 µM) was added to the well containing probe **X** and incubated at 4 °C on ice for 15 min (Final probe concentration = 2 µM). The plate was irradiated at 365 nm for 10 min and 20 min on ice. The plate was sealed, centrifuged (1000 rpm, 1 min) and sampled directly for intact protein LC-MS analysis using the methods described in SI Section 4.1. This experiment was performed for all 12 probes (**P1-P12**) against CDK2 recombinant protein in duplicate.

4.2.1 Data tables of photocrosslinking yields for probes **P1-P12** against CDK2 recombinant protein

SI Table 11: Crosslinking yields of probe **P1-P12** against CDK2

	20 min		**10 min**	
Probe	**Mean**	**SD**	**Mean**	**SD**
P1	0.00	0.00	0.00	0.00
P3	0.00	0.00	0.00	0.00
P5	0.00	0.00	0.00	0.00
P7	0.00	0.00	0.00	0.00
P9	0.79	0.15	0.00	0.00

P2	0.00	0.00	0.00	0.00
P4	1.7	0.15	1.03	0.06
P6	2.88	0.17	1.70	0.39
P8	0.00	0.00	0.00	0.00
P10	0.00	0.00	0.00	0.00
P11	1.18	0.18	0.00	0.00
P12	6.14	0.73	3.56	0.10

4.4 Identification of site of crosslinking of **P12** by LC-MS/MS analysis

4.4.1 Method

CDK2 protein provided under Genescript/GSK collaboration: 6H-Flag-Tev-CDK2 (41 µM).

Samples of CDK2 protein (3 µM) incubated with **P12** (6 µM) or DMSO and irradiated for 5 min at 302nm in 50 mM HEPES buffer were prepared and subjected to an in-solution tryptic digest followed by LC-MS/MS analysis using a Q-Exactive mass spectrometer. Tryptic digestion and LC-MS/MS analysis were carried out in duplicate.
Each sample (27 µL) was diluted with 100 mM ammonium bicarbonate (13 µL) to a final concentration of 2 µM. Samples were reduced using TCEP (final concentration 0.125 mM) and incubated for 20 min at 65 °C. Upon cooling iodoacetamide was added to a final concentration of 10 mM and the samples were incubated for 20 min at rt in the dark. Trypsin (2.5 µL, 20 ng/µL, Promega) in 100 mM ammonium bicarbonate was added for a 1:60 *w/w* and incubated for 3 hrs at 37 °C. The reaction was stopped with the addition of 1% formic acid (5 µL). Digested samples were injected on an Easy nLC1000 UHPLC system (Thermo Scientific). The nanoLC was interfaced to a Q-Exactive Hybrid Quadrupole-Orbitrap Mass Spectrometer (Thermo Scientific). Tryptic peptides were separated on a 25cm x 75µm ID, Acclaim PepMap C18, 3 µm particle column (Thermo Scientific) using a 40 min gradient of 2-30% acetonitrile/0.2% formic acid and a flow of 300 nL/min. MS-based peptide sequencing data were acquired using data dependent LC-MS/MS (top 10 method, scan range 400-2000 m/z, resolution 70,000, AGC target 1e6). HCD MS/MS spectra were acquired at a resolution of 17500 (AGC target 5e4). The normalised collision energy (CE) for HCD was set to either 27 or 30. Alternatively, samples were analysed with a Parallel Reaction Monitoring (PRM) method using a 1.0 m/z isolation window on the precursor value and a CE of either 27 or 30.

4.4.2 Analysis

Uninterpreted spectra were searched for peptide matches against the Genescript/GSK CDK2 sequence using the Mascot software (Version 2.6.0) (Matrix Science) using a 5 ppm mass tolerance for peptide precursors and 20 mDa mass tolerance for fragment ions. Oxidation (M) and **P12** modification on any residue were allowed as variable modifications and carbamidomethylation (C) was used as a fixed modification.
Mascot results showed a CDK2 sequence coverage of ca. 75-90% and suggested **P12** crosslinking occurring on peptide 11-22, possibly on residue K20. No modification was detected in the DMSO control sample. To confirm site assignement, samples were analysed using an LC-MS/MS PRM method targeting **P12**-modified and unmodified peptide 11-22. Manual validation of the PRM data confirmed crosslinking of **P12** at K20.

5. MS-based proteomics

5.1 Biochemistry for cell lysate pulldown

Preparation of lysate
3 volumes of chilled lysis buffer (50 mM HEPES, 5% glycerol, 1.5 mM $MgCl_2$, 150 mM NaCl, 1 mM Na_3VO_4, 0.8% IGEPAL CA-630, 25 mM NaF, 1x PIM5 (in-house protease inhibitor mix containing 500 nM Aprotinin (Sigma, A1153), 40 µM Bestatin (Sigma, B8386), 100 µM Leupeptin (Sigma, L2884), 1.46 µM Pepstatin (Sigma, P5318), 10 µM Phosphoramidon (Sigma, R7386)) was added to one volume of HL-60 cell pellet and the mixture was rotated overhead (15 min , 4 °C). The cell suspension was homogenised using a Wheaton Dounce tissue grinder (Sartorius) before mixing by overhead rotation (30 min, 4 °C). The mixture was centrifuged (20,000 × g, 10 min, 4 °C) and the supernatant was transferred and centrifuged (140,000 × g, 1 h, 4 °C). The supernatant was aliquoted and flash-frozen. The protein concentration was determined by BCA assay (Pierce BCA protein assay kit, Thermo Scientific, 23225, using Quick Start BSA Standard Set, Bio-Rad, 500-0207).

PAL labelling and pulldown
2.0 mL of HL-60 lysate (17.4 mg/mL, 2.0 mL) was diluted with 50 mM HEPES, 5% glycerol, 1.5 mM $MgCl^2$, 150 mM NaCl, 25 mM NaF, 1x PIM5 (2.0 mL) to reduce the IGEPAL CA-630 concentration from 0.8% to 0.4%. The lysate was further diluted with 50 mM HEPES, 5% glycerol, 1.5 mM $MgCl_2$, 150 mM NaCl, 25 mM NaF, 0.4% IGEPAL CA-630, 1x PIM5 to a final protein concentration of 1.5 mg/mL. Diluted lysate (1.5 mg/mL, 3.0 mL) was added to wells A1 and A2 of a 6-well plate (Corning, CLS3516) on ice. **P12** (2.0 mM in DMSO, 15 µL, FAC = 10 µM) was added to both wells. DMSO (15 µL) was added additionally to A1. Competitor **9** (40 mM, 15 µL, FAC = 200 µM) was added additionally added to A2. The plate was mixed by gentle rotary shaking (1 h, 4 °C). The samples were irradiated on ice (302 nm, 10 min, UVP photocrosslinking lightbox, CL-1000M). The bulbs were warmed for 2 min prior to sample irradiation. Each sample (2.5 mL) was transferred to a 5 mL eppendorf vial, and 275 µL of a CuAAC click mix containing $CuSO_4$ (50 mM in water, 50 µL, Sigma, C8027), TBTA ligand (1.7 mM in 1:4 (v/v) DMSO:t butanol, 150 µL, Sigma,

678937), biotin-azide (10 mM in DMSO, 25 µL, TCI, A2523) and freshly prepared TCEP (50 mM in water, 50 µL, Sigma, C4706) was added. The vials were mixed by overhead rotation (rt, 1 h). To 2.0 mL of each sample, acetone (8.0 mL, pre-chilled to -25 °C) was added and the samples were briefly vortexed before being stored at -25 °C for 1.5 h. The samples were centrifuged (16000 × g, 10 min, 4 °C) and the supernatant was aspirated. 4:1 (v/v) acetone:water (10 mL, -25 °C) was added and the samples were centrifuged (16000 × g, 10 min, 4 °C). The supernatant was aspirated and 2.5 M urea in 50 mM HEPES, 5% glycerol, 1.5 mM $MgCl_2$, 150 mM NaCl, 25 mM NaF, 0.4% IGEPAL CA-630, 1x PIM5 (400 µL) was added. The samples were sonicated (ca. 5 min) and 20% SDS (16 µL) was added. The samples were further sonicated (ca. 1 min) before being diluted with 50 mM HEPES, 5% glycerol, 1.5 mM $MgCl_2$, 150 mM NaCl, 25 mM NaF, 0.4% IGEPAL CA-630, 1x PIM5 (1.6 mL) to give a final concentration of 0.5 M urea and 0.16% SDS. The samples were split into 2 × 1 mL replicates, and each 1 mL replicate was incubated (overhead rotation, 4 °C, 2 h) with neutravidin beads (35 µL dry bead volume, Pierce high capacity neutravidin beads, Thermo Scientific, 29204) which were pre-washed with PBS. Each replicate was filtered (96 well filter plates, Porvair Sciences, 600033) and washed with 50 mM HEPES, 5% glycerol, 1.5 mM $MgCl_2$, 150 mM NaCl, 25 mM NaF, 0.4% IGEPAL CA-630 (10 × 1 mL) and 50 mM HEPES, 5% glycerol, 1.5 mM $MgCl_2$, 150 mM NaCl, 25 mM NaF, 0.2% IGEPAL CA-630 (5 × 1 mL). The samples were then incubated (50 °C, 30 min, 750 rpm rotary shaking) with 0.5x NuPAGE LDS sample buffer (Thermo Scientific, NP0007) containing 50 mM DTT (50 µL). The samples were filtered and further washed with 50 mM HEPES, 400 mM NaCl, 0.5% SDS (5 × 1 mL), 50 mM HEPES, 400 mM NaCl (10 × 1 mL), 50 mM HEPES, 2 M urea (10 × 1 mL) and 50 mM HEPES (5 × 1 mL). 60 µL of an on-bead digestion mix containing 40 mM HEPES, 15 mM 2-chloroacetamide (Sigma, 22790), 5 mM TCEP, 4 ng/µL LysC (Wako Chemicals, 125-05061), 4 ng/µL Trypsin (Promega, V5111) was added and the samples were incubated overnight (rt, 750 rpm rotary shaking). The digests were filtered and the retentate was washed with 50 mM HEPES (60 µL). The combined filtrate was frozen (-80 °C), lyophilised and stored at -20 °C.

5.2 Analysis for cell lysate pulldown

Lyophilized peptides were resuspended in HPLC grade water then labelled with isobaric mass-tag (TMT6, Thermo Fisher Scientific) reagents and quenched with hydroxylamine. Labelled peptide extracts were combined to a single sample per experiment. Combined samples were then desalted using C18-SCX stage tips: for each stage tip, 3 plugs SCX material (Cation 47 mm Extraction Disks 2252, Empore/3M) were overlaid with 3 plugs C18 material (Octadecyl C18 47 nm Extraction Disks, Empore/3M). After equilibration with 0.5% trifluoroacetic acid (TFA) 2% acetonitrile, combined samples were loaded on the stage tips. Stage tips were washed with 0.5% TFA in 2% acetonitrile, and twice with 0.5% TFA in 60% acetonitrile, followed by elution of bound peptides with 5% ammonia in 80% acetonitrile. Desalted peptides were dried in vacuo and resuspended in 0.05% trifluoroacetic acid in water and injected into an Ultimate3000 nanoRLSC (Dionex, Sunnyvale, CA) coupled to a Q-Exactive HF (Thermo Fisher Scientific).

Peptides were separated on custom 50 cm × 100 µM (ID) reversed-phase columns (Reprosil) at 40 °C. Gradient elution was performed from 2% to 40% acetonitrile in 0.1% formic acid over 200 minutes. Samples were online injected into a Q-Exactive Plus mass spectrometer operating with a data-dependent top 10 method. MS spectra were acquired by using 70.000 resolution and an ion target of 3E6. Higher energy collisional dissociation (HCD) scans were performed with 33% NCE at 35.000 resolution (at m/z 200), and the ion target setting was set to 2E5 to avoid coalescence. Sample was measured twice and both runs were combined for analysis.

Mascot 2.5 (Matrix Science) was used for protein identification by using a 10 ppm mass tolerance for peptide precursors and 20 mDa (HCD) mass tolerance for fragment ions. Carbamidomethylation of cysteine residues and TMT modification of lysine residues were set as fixed modifications. N-terminal acetylation of proteins and TMT modification of peptide N-termini were set as variable modifications.

Swissprot human (downloaded on January 2018) was used as search database, combined with a decoy version of this database created by using a script supplied by MatrixScience. We accepted protein identifications as follows: (i) For single-spectrum to sequence assignments, we required this assignment to be the best match and a minimum Mascot score of 31 and a 10× difference of this assignment over the next best assignment. Based on these criteria, the decoy search results indicated <1% false discovery rate (FDR). (ii) For multiple spectrum to sequence assignments and using the same parameters, the decoy search results indicate <0.1% FDR. All identified proteins were quantified; FDR for quantified proteins was <1%. For the analysis an in house version of isobarQuant 1 was used.[6]

6. Photoaffinity displacement assay

Irradiation and LC-MS analysis was carried out following the general experimental procedure described previously in SI Section 4.1.

6.1 Photoaffinity displacement assay experimental

Example procedure: 300 nL of competitor compound (variable concentration in DMSO) was transferred into a Greiner 384 low volume plate (784076) using a Labcyte Echo 555 Liquid Handler®. 15 µL of a solution containing CDK2 protein (6H-Flag-Tev-CDK2, 1 µM)/**P12** (5 µM) in buffer (50 mM HEPES, 10 mM $MgCl_2$) was added to the wells containing competitor compound and incubated at 4 °C for 15 min. The plate was irradiated at 302 nm for 10 min on ice. The plate was sealed, centrifuged (1000 rpm, 1 min) and sampled directly for intact protein LC-MS analysis using the methods described in SI Section 4.1. This experiment was performed for compounds **1** and **17**-**35** against CDK2 recombinant protein in triplicate.

6.1.1 Data tables of crosslinking yields of **P12** in the displacement assay

The crosslinking yields of **P12** in the displacement assay were extracted using the method described in SI Section 4.1. Crosslinking yields for each well were normalised to the DMSO control for that row.

The following data tables detail the normalised crosslinking yields. These values were plotted in Graphpad Prism 5.0.4 software to generate dose response curves and IC_{50} values. Lines were fitted with non-linear regression using 'log(inhibitor) vs response (three parameters)'. The curves were constrained to have a maximum of 1 and a minimum of 0.

SI Table 12: Normalised crosslinking yields of the 20 competitive inhibitors in triplicate.

	1, roscovitine			17		
Concentration of competitive inhibitor (μM)	**T1**	**T2**	**T3**	**T1**	**T2**	**T3**
200	0.22	0.21	0.22	0.84	1.16	1.28
100	0.27	0.26	0.27	0.94	1.22	1.14
50	0.32	0.33	0.34	1.00	1.22	1.10
25	0.38	0.42	0.42	1.01	1.07	1.00
12.5	0.37	0.41	0.43	0.99	1.12	1.07
6.25	0.51	0.51	0.56	0.99	1.16	0.95
3.13	0.58	0.55	0.64	0.99	1.07	0.98
1.56	0.68	0.69	0.68	1.01	1.05	0.96
0	1.00	1.00	1.00	1.00	1.00	1.00

	18			19		
Concentration of competitive inhibitor (μM)	**T1**	**T2**	**T3**	**T1**	**T2**	**T3**
200	0.43	0.79	0.62	0.51	0.76	0.86
100	0.57	0.69	0.75	0.62	0.76	1.05
50	0.72	0.78		0.74	0.91	1.05
25	0.78	0.85	0.74	0.84	0.92	1.04
12.5	0.85	0.95	0.60	0.89	1.03	1.01
6.25		1.07		0.94	0.99	1.06
3.13	0.93	1.07	0.63	1.00	1.06	1.08
1.56	0.96	1.06	0.80	1.00	1.09	1.09
0	1.00	1.00		1.00	1.00	1.00

	20			21		
Concentration of competitive inhibitor (μM)	**T1**	**T2**	**T3**	**T1**	**T2**	**T3**
200	0.84	1.04	1.00	0.28	0.29	0.29
100	0.96	1.16	1.11	0.32	0.31	0.33
50	0.99	1.22	1.24	0.39	0.38	0.38
25	1.03	1.16	1.15	0.51	0.47	0.47
12.5	1.05	1.12		0.67	0.60	0.62
6.25	1.03	1.11	1.06	0.79	0.78	0.81
3.13	1.03	1.10		0.90	0.86	0.85
1.56	1.02	1.09	1.09	0.99	0.91	0.93
0	1.00	1.00	1.00	1.00	1.00	1.00

	22			23		
Concentration of competitive inhibitor (μM)	**T1**	**T2**	**T3**	**T1**	**T2**	**T3**
200	0.24	0.25	0.28	0.25	0.35	0.35
100	0.24	0.26	0.25	0.23	0.28	0.34
50	0.25	0.28	0.26	0.28	0.28	0.32
25	0.33	0.30	0.30	0.33	0.31	0.36
12.5	0.42	0.39	0.41	0.43	0.40	0.41
6.25	0.60	0.53	0.59	0.58	0.54	0.56
3.13	0.72	0.64	0.69	0.71	0.65	0.71
1.56	0.83	0.75	0.79	0.84	0.79	0.84
0	1.00	1.00	1.00	1.00	1.00	1.00

	24			25		
Concentration of competitive inhibitor (μM)	**T1**	**T2**	**T3**	**T1**	**T2**	**T3**
200	0.39	0.43	0.47	0.76	0.70	0.84
100	0.42	0.44	0.48	0.83	0.74	0.84
50	0.53	0.55	0.55	0.92	0.86	0.88
25	0.65	0.69	0.68	0.97	0.94	0.85
12.5	0.77	0.82	0.79	1.00	0.98	0.93
6.25	0.86	0.89	0.91	1.04	0.96	0.93
3.13	0.91	0.91	0.93	1.07	0.99	0.99
1.56	0.92	0.96	0.98	1.08	0.95	1.06
0	1.00	1.00	1.00	1.00	1.00	1.00

	26, BS-181			27		
Concentration of competitive inhibitor (μM)	**T1**	**T2**	**T3**	**T1**	**T2**	**T3**
200		0.47	0.47		0.17	0.18
100	0.69	0.67	0.72	0.22	0.23	0.24
50	0.81	0.79	0.91	0.24	0.25	0.28
25	0.91	0.88	1.02	0.32	0.34	0.40
12.5	0.95	0.88	1.13	0.28	0.32	0.33
6.25	0.96	0.90	1.16	0.41	0.49	0.53
3.13	0.96	0.91	1.20	0.49	0.52	0.65
1.56	0.98	0.93	1.20	0.54	0.56	0.67
0	1.00	1.00	1.00	1.00	1.00	1.00

	28			29, AT7519		
Concentration of competitive inhibitor (μM)	**T1**	**T2**	**T3**	**T1**	**T2**	**T3**
200	0.25	0.27	0.27	0.20	0.19	0.33
100	0.25	0.27	0.26	0.19	0.19	0.35
50	0.25	0.27	0.27	0.18	0.17	0.35
25	0.28	0.29	0.27	0.21	0.19	0.37

12.5	0.34	0.37	0.34	0.20	0.19	0.37
6.25	0.45	0.47	0.48	0.20	0.21	0.37
3.13	0.56	0.60	0.56	0.24	0.20	0.38
1.56	0.71	0.73	0.75	0.20	0.21	0.41
0	1.00	1.00	1.00	1.00	1.00	1.00

		30			**31**	
Concentration of competitive inhibitor (μM)	**T1**	**T2**	**T3**	**T1**	**T2**	**T3**
200	0.38	0.67		0.15	0.18	0.17
100	0.24	0.39	0.32	0.16	0.18	0.18
50	0.19	0.29	0.27	0.17	0.18	0.19
25	0.19	0.23	0.26	0.18	0.20	0.19
12.5	0.18	0.23	0.22	0.22	0.22	0.22
6.25	0.19	0.22	0.21	0.28	0.26	0.26
3.13	0.19	0.35	0.20	0.35	0.35	0.32
1.56	0.21	0.24	0.22	0.44	0.44	0.44
0	1.00	1.00	1.00	1.00	1.00	1.00

		32			**33**	
Concentration of competitive inhibitor (μM)	**T1**	**T2**	**T3**	**T1**	**T2**	**T3**
200	0.32	0.30		0.34	0.35	0.41
100	0.18	0.27		0.25	0.34	0.33
50	0.16	0.24	0.34	0.24	0.31	0.32
25	0.15	0.25	0.27	0.25	0.29	0.28
12.5	0.17	0.20		0.30	0.35	0.37
6.25	0.20	0.22	0.23	0.38	0.39	0.39
3.13	0.24	0.25	0.27	0.50	0.49	0.52
1.56	0.31	0.31	0.33	0.66	0.64	0.65
0	1.00	1.00	1.00	1.00	1.00	1.00

		34, flavopiridol			**35, R457**	
Concentration of competitive inhibitor (μM)	**T1**	**T2**	**T3**	**T1**	**T2**	**T3**
200	0.19		0.21	0.18	0.17	0.18
100	0.20	0.22	0.22	0.17	0.17	0.18
50	0.21	0.21	0.24	0.17	0.16	0.20
25	0.22	0.24		0.17	0.16	0.19
12.5	0.25	0.27	0.28	0.17	0.17	0.18
6.25	0.29	0.32	0.38	0.17	0.17	0.19
3.13	0.34	0.36	0.43	0.16	0.17	0.19
1.56	0.48	0.51	0.54	0.16	0.17	0.17
0	1.00	1.00	1.00	1.00	1.00	1.00

Blank wells arose from failure to inject on the MS. This data generated the following pIC_{50} values for each of the competitive inhibitors (**SI Table 13**). The compounds were also tested in the ADP-Glo™ assay and this data is also included in the table. A modified Cheng-Prusoff equation was used to correct the pIC_{50} values generated in the photoaffinity displacement assay on to the same scale as the ADP-Glo™ assay, using the ADP-Glo™-derived pIC_{50} of **P12**.

$$\text{Cheng-Prusoff: } K_i = IC_{50} / (1 + [S] / K_m)$$

$$\text{Modified Cheng-Prusoff: } IC_{50} \text{ competitor} = IC_{50} / (1 + [\mathbf{P12}] / IC_{50}\ \mathbf{P12})$$

SI Table 13: Comparison of pIC_{50} values in photoaffinity and ADP-Glo™ assays

Compound	**Photoaffinity assay (pIC_{50})**	**Cheng-Prusoff corrected Photoaffinity assay (pIC_{50})**	**ADP-Glo™ assay (pIC_{50})**
20	>6/0	>7.4	5.1
30	>6.0	>7.4	7.3
35, R547	>6.0	>7.4	9.2
29, AT7519	>6.0	>7.4	7.6
32	>6.0	>7.4	7.1
31	>6.0	>7.4	6.8
34, flavopiridol	6.0	7.4	7.8
33	5.9	7.3	7
27	5.6	7.0	6.1
28	5.6	7.0	6.1
1, roscovitine	5.6	7.0	6.7
23	5.4	6.8	7.1
22	5.3	6.7	7.1
21	4.8	6.2	6.6

17	4.7	6.1	5.6
24	4.6	6.0	5.5
18	4.6	6.0	6
25	4.0	5.4	5.3
26, BS-181	3.6	5.0	6
19	3.5	4.9	5.7

7. 1H NMR Spectra of P1-P12

^{1}H NMR of **P1**

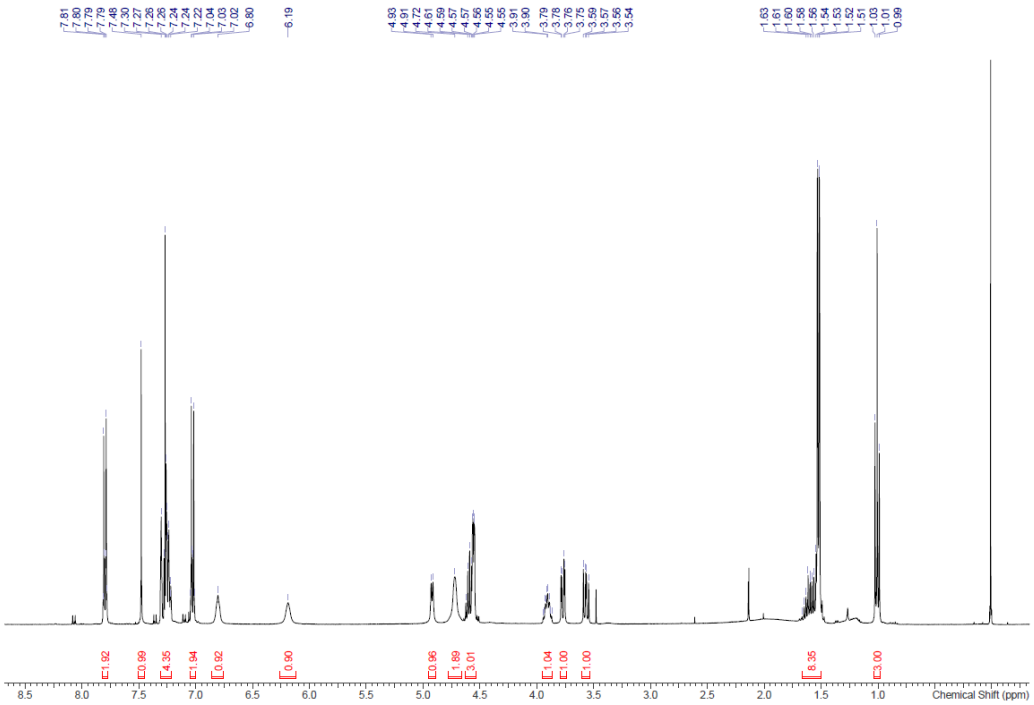

^{1}H NMR of **P2**

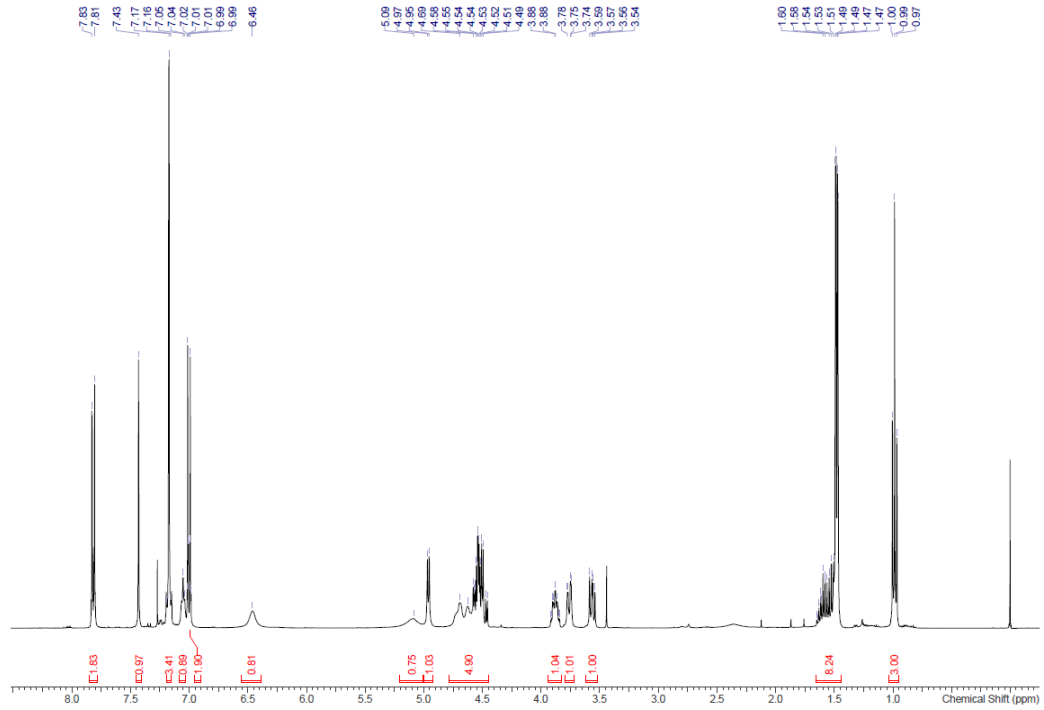

^{1}H NMR of **P3**

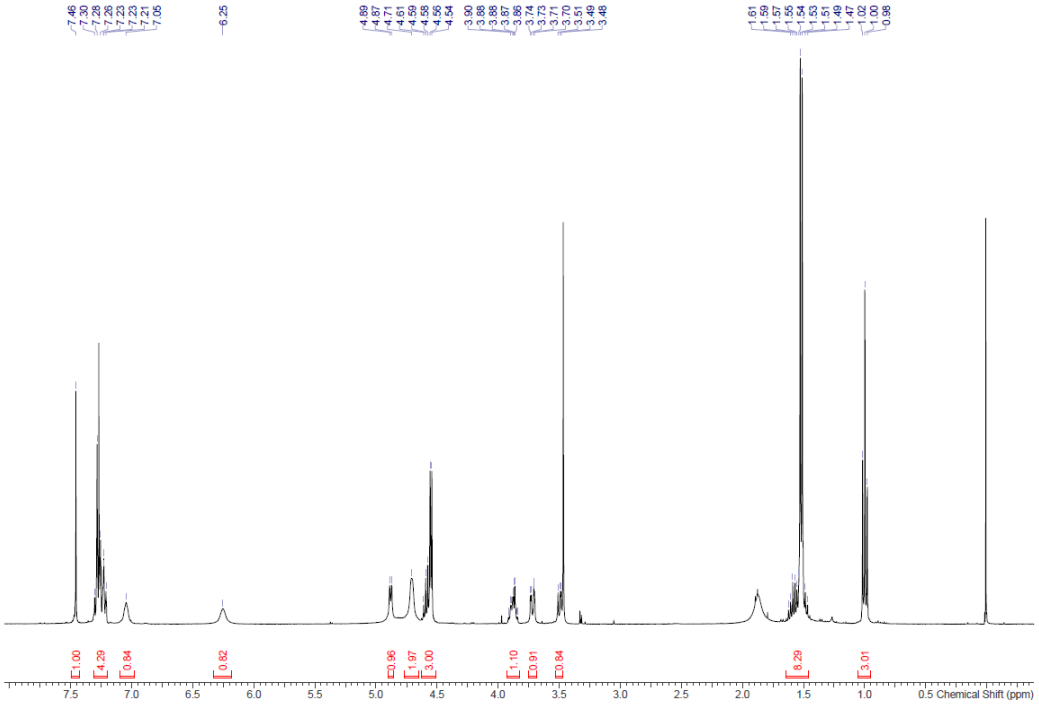

^{1}H NMR of **P4**

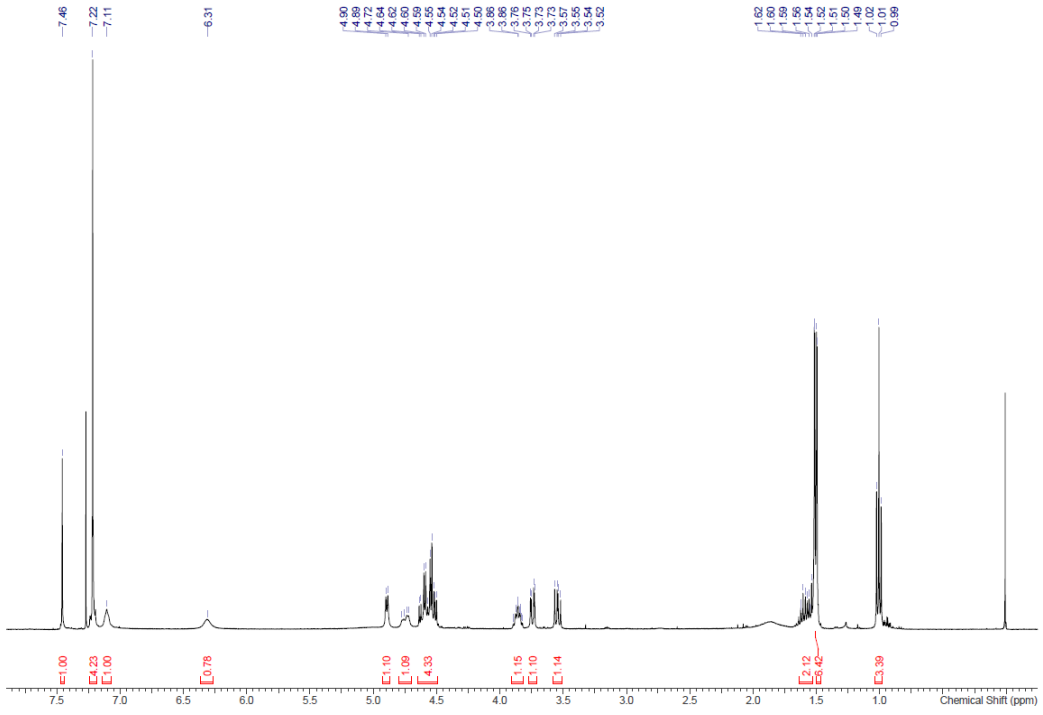

^{1}H NMR of **P5**

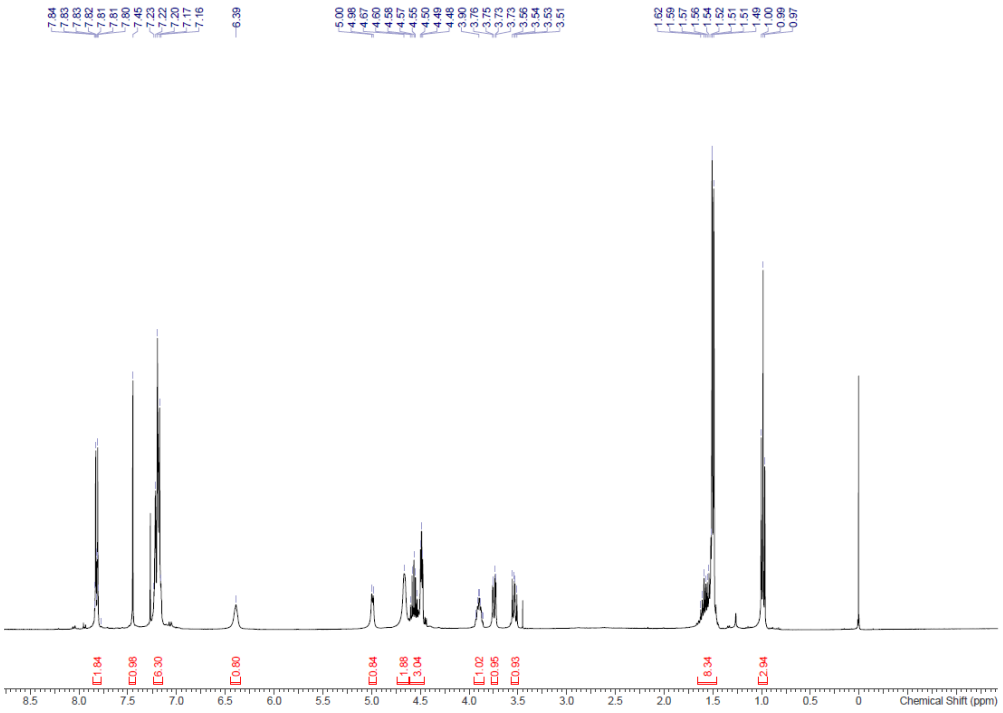

^{1}H NMR of **P6**

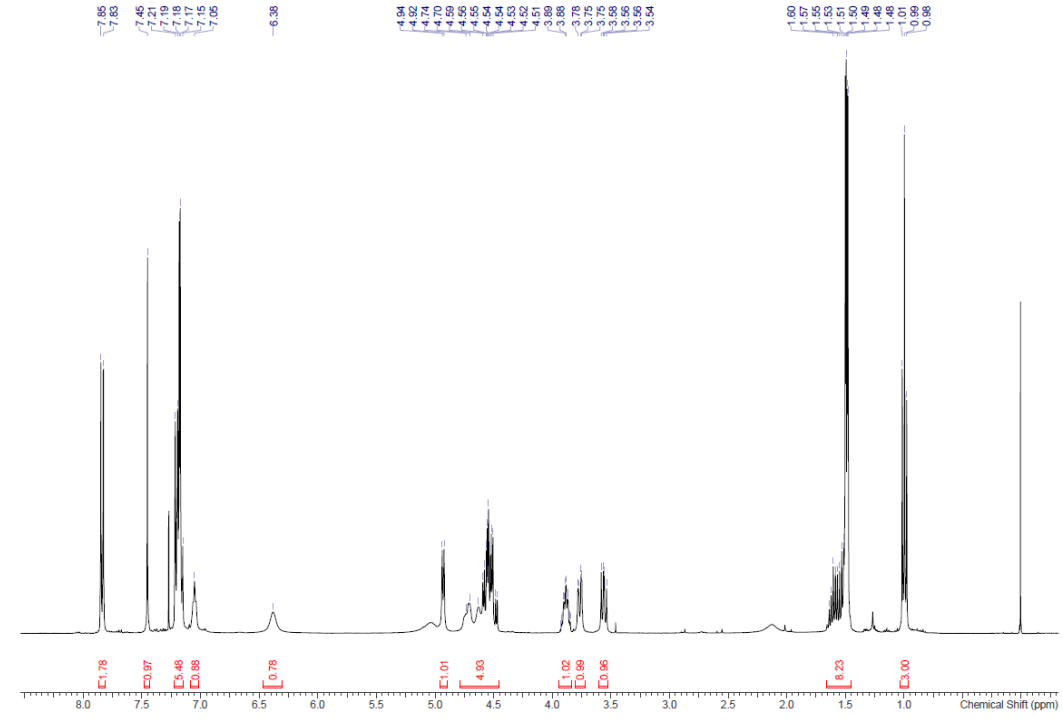

^{1}H NMR of **P7**

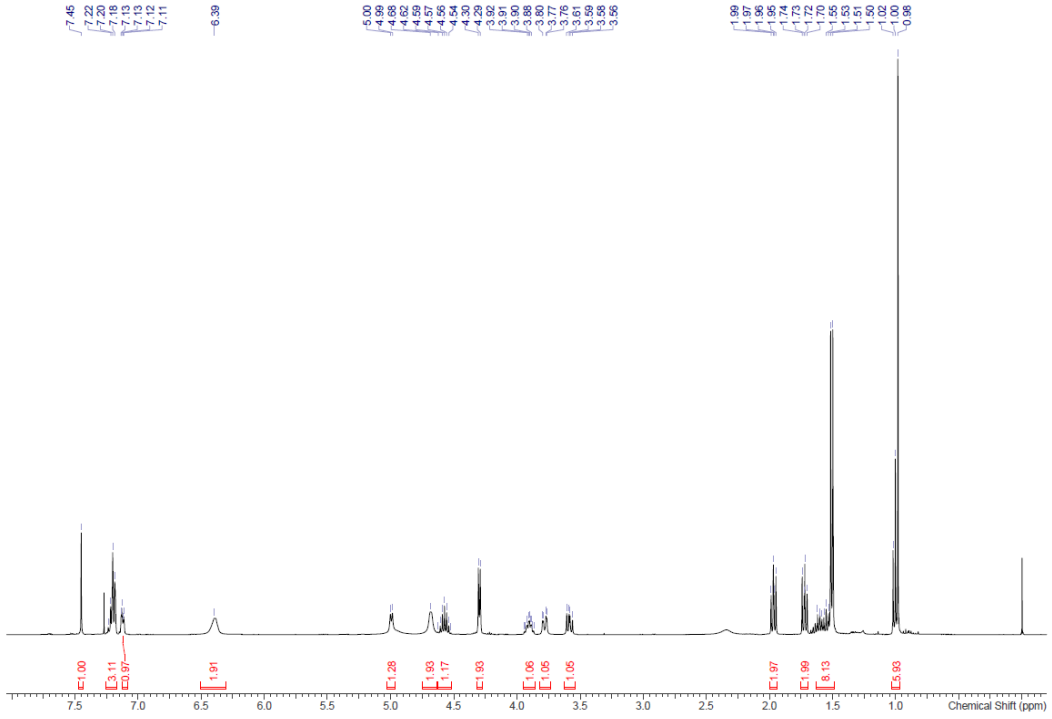

^{1}H NMR of **P8**

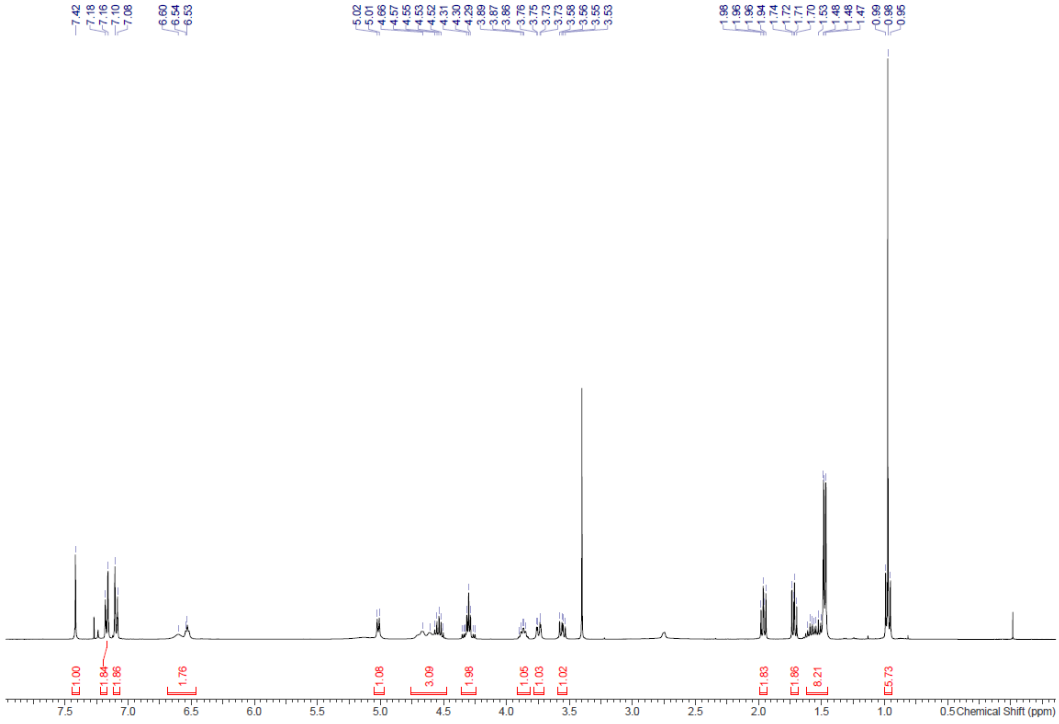

^{1}H NMR of **P9**

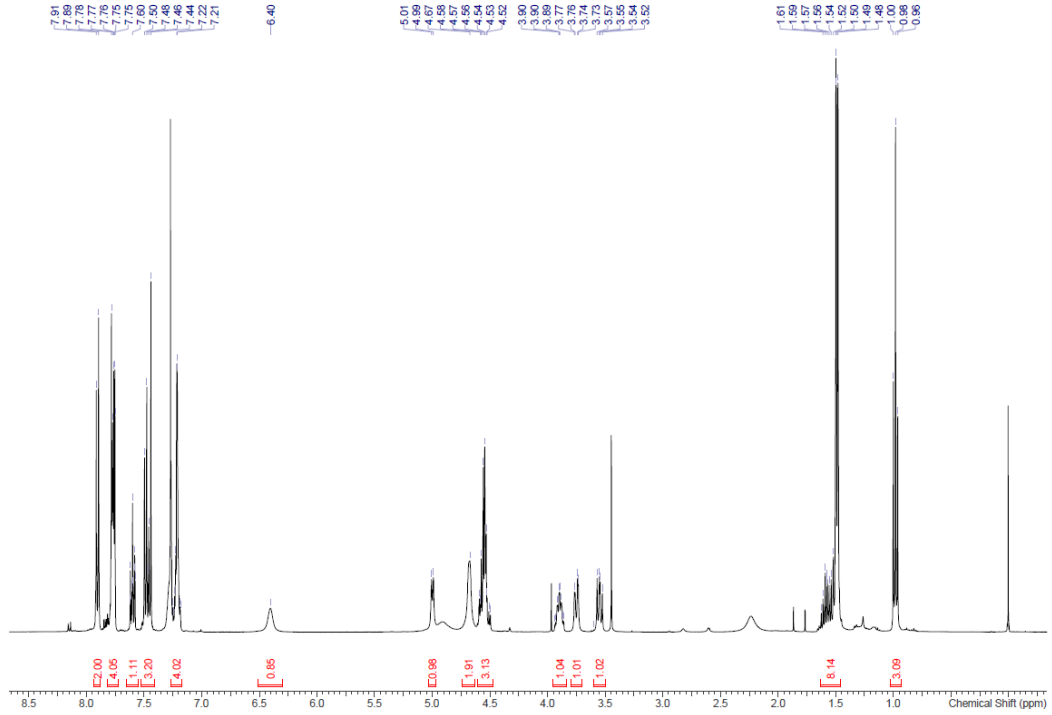

^{1}H NMR of **P10**

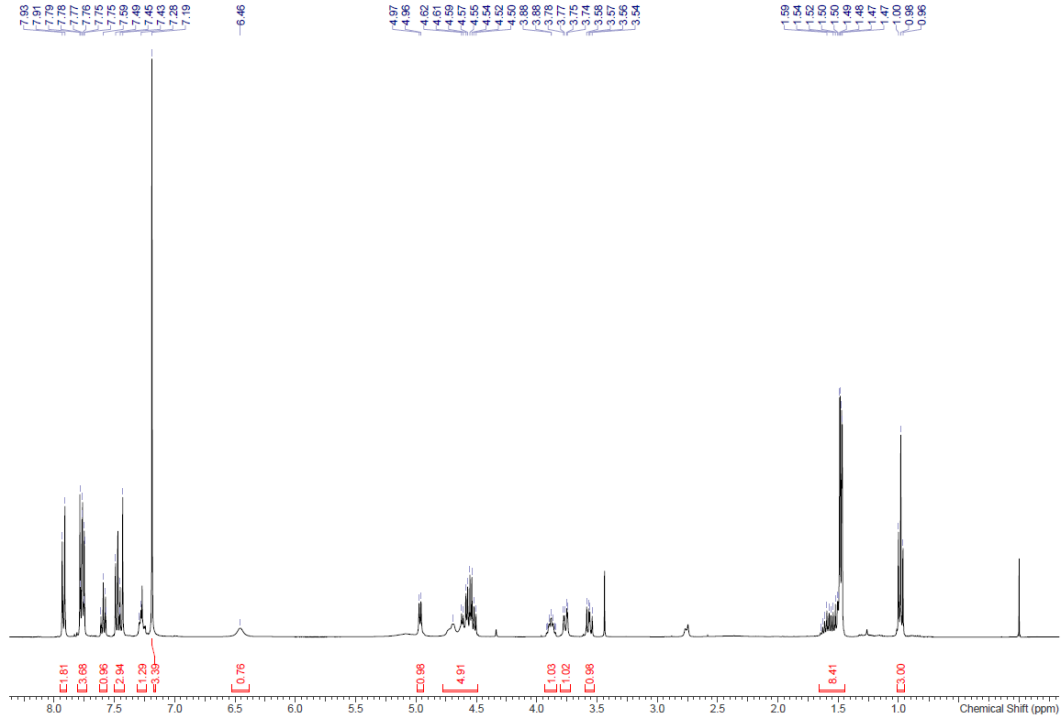

^{1}H NMR of **P11**

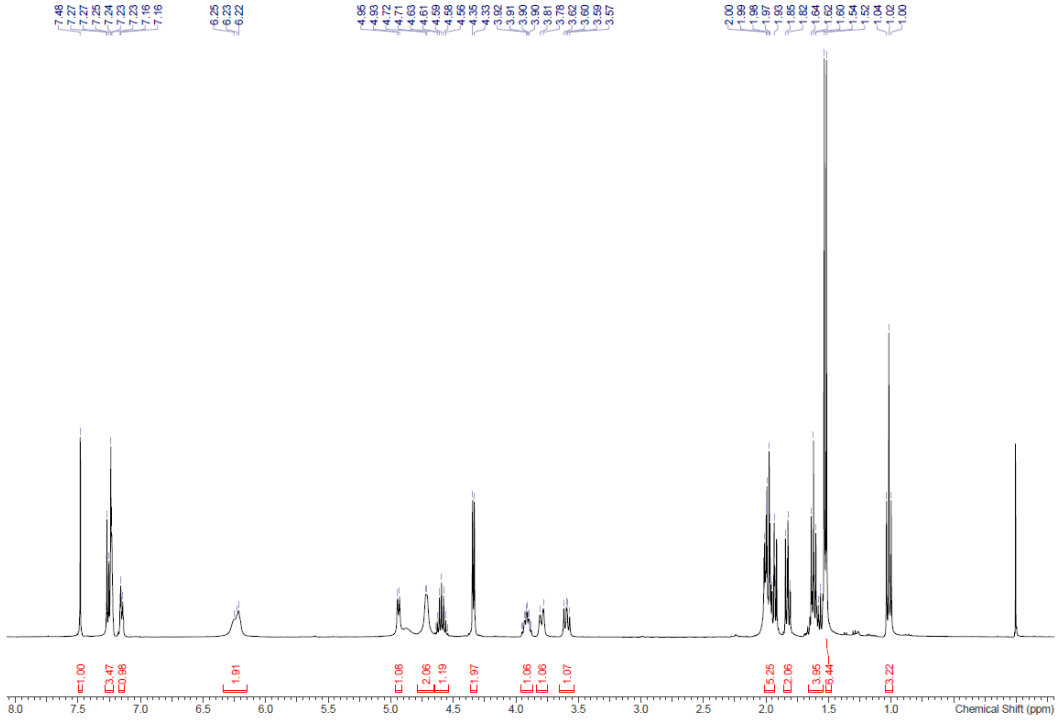

^{1}H NMR of **P12**

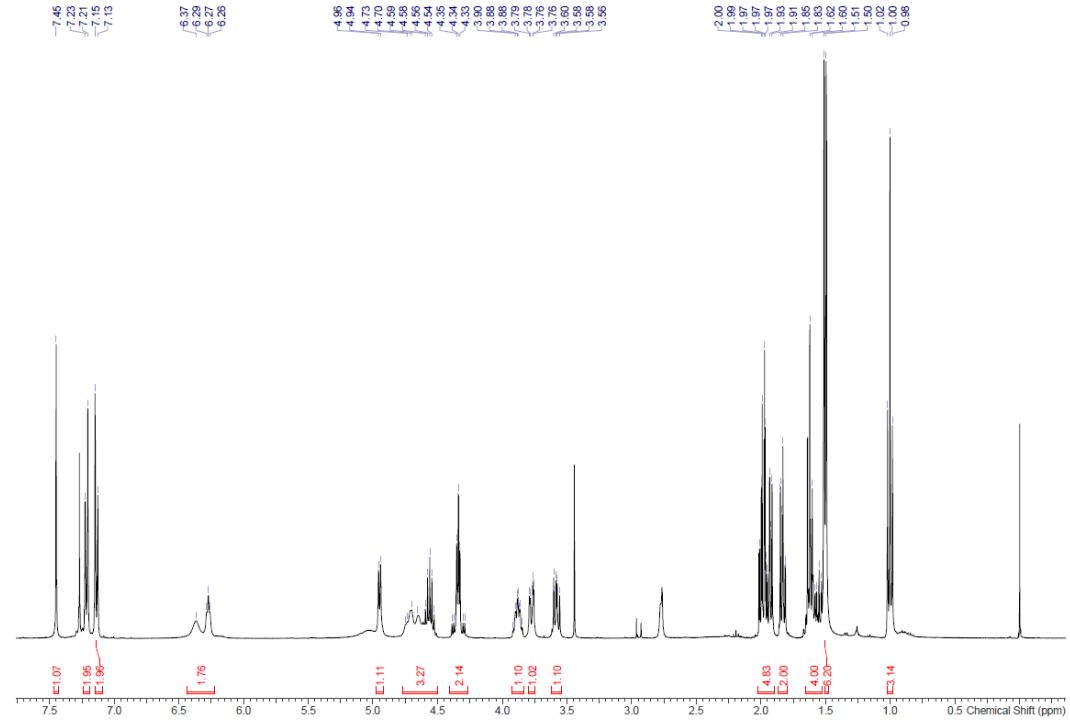

8. References

[1] G. Camurri, A. Zaramella, *Anal. Chem.* **2001**, *73*, 3716-3722.
[2] K. Valko, S. Nunhuck, C. Bevan, M. H. Abraham, D. P. Reynolds, *J. Pharm. Sci.* **2003**, *92*, 2236-2248.
[3] K. Valko, *Physicochemical and Biomimetic Properties in Drug Discovery:Chromatographic Techniques for Lead Optimization*, Wiley, **2014**.
[4] M. W. Robinson, A. P. Hill, S. A. Readshaw, J. C. Hollerton, R. J. Upton, S. M. Lynn, S. C. Besley, B. J. Boughtflower, *Anal. Chem.* **2017**, *89*, 1772-1777.
[5] L. Ballell, R. H. Bates, R. J. Young, D. Alvarez-Gomez, E. Alvarez-Ruiz, V. Barroso, D. Blanco, B. Crespo, J. Escribano, R. Gonzalez, S. Lozano, S. Huss, A. Santos-Villarejo, J. J. Martin-Plaza, A. Mendoza, M. J. Rebollo-Lopez, M. Remuinan-Blanco, J. L. Lavandera, E. Perez-Herran, F. J. Gamo-Benito, J. F. Garcia-Bustos, D. Barros, J. P. Castro, N. Cammack, *Chem. Med. Chem.* **2013**, *8*, 313-321.
[6] H. Franken, T. Mathieson, D. Childs, G. M. Sweetman, T. Werner, I. Togel, C. Doce, S. Gade, M. Bantscheff, G. Drewes, F. B. Reinhard, W. Huber, M. M. Savitski, *Nat. Protoc.* **2015**, *10*, 1567-1593.

Author Contributions

Emma K. Grant was lead contributor to all experimental work, analysis of compounds, analysis of LC-MS results, and equal contributor to writing of the original draft.
David. J. Fallon contributed equally to MS-based proteomics experimental work and analysis.
H. Christian Eberl was the lead contributor to the analysis of MS-based proteomics.
Ken G.M. Fantom was equal contributor to the preparation and analysis of LC-MS/MS results.
Francesca Zappacosta was equal contributor to the analysis of LC-MS/MS results.
Cassie Messenger was the lead contributor to the collection and analysis of ADP-Glo data.
Nicholas C.O. Tomkinson was the supporting contributor to the writing of the original draft.
Jacob T. Bush was equal contributor to interpretation of all results and writing of the original draft.